Applied Catalysis B: Environmental 343 (2024) 123454

Contents lists available at ScienceDirect

Applied Catalysis B: Environmental

journal homepage: www.elsevier.com/locate/apcatb

Interpretable machine learning framework for catalyst performance prediction and validation with dry reforming of methane

Jiwon Roh [a,b], Hyundo Park [a,b], Hyukwon Kwon [a,b], Chonghyo Joo [a,b], Il Moon [a], Hyungtae Cho [b], Insoo Ro [c,*], Junghwan Kim [a,*]

[a] Department of Chemical and Biomolecular Engineering, Yonsei University, Seoul 03722, Republic of Korea
[b] Green Materials and Processes R&D Group, Korea Institute of Industrial Technology, Ulsan 44413, Republic of Korea
[c] Department of Chemical and Biomolecular Engineering, Seoul National University of Science and Technology, Seoul 01811, Republic of Korea

ARTICLE INFO

Keywords:
Interpretable machine learning
Dry reforming of methane
Shapley additive explanation
Partial dependence value
Catalyst

ABSTRACT

Conventional methods for developing heterogeneous catalysts are inefficient in time and cost, often relying on trial-and-error. The integration of machine-learning (ML) in catalysis research using data can reduce computational costs and provide valuable insights. However, the lack of interpretability in black-box models hinders their acceptance among researchers. We propose an interpretable ML framework that enables a comprehensive understanding of the complex relationships between variables. Our framework incorporates tools such as Shapley additive explanations and partial dependence values for effective data preprocessing and result analysis. This framework increases the prediction accuracy of the model with improved R^2 value of 0.96, while simultaneously expanding the catalyst component variety. Furthermore, for the case of dry reforming of methane, we tested the validity of the catalyst recommendation through dedicated experimental tests. The outstanding performance of the framework has the potential to expedite the rational design of catalysts.

1. Introduction

The development of heterogeneous catalysts has mainly relied on experimental trial-and-error based on experts' insights [1]. However, this method is inefficient when exploring a large parameter space with complex variables, and it has limitations in terms of the cost and time constraints for conducting experiments. Therefore, statistical approaches such as design of experiments (DOE) and computational chemistry calculations such as density functional theory (DFT) and molecular dynamics have been used to design experiments or calculate the energy changes of transition states based on the reaction mechanism [2,3]. Although DOE is useful for exploring optimal operating conditions in the design space, experiments must be conducted with the same time and cost limitations. However, computational chemistry approaches have shown promising results in many studies, they require complexity and computational cost because of the analysis of the energy transitions for each transition state in the reaction mechanism. Furthermore, the synthesis and experimental reproduction of catalysts with specific facets or structures pose significant technical difficulties, even when optimal combinations are derived [4].

The process of CH_4 reforming with CO_2, also known as dry reforming of methane (DRM), has gained considerable attention owing to its potential as a promising pathway for simultaneously converting two major greenhouse gases into syngas (H_2 and CO) [5]. Syngas is a highly valuable intermediate in chemical synthesis. Currently, steam reforming of methane accounts for over 95% of conventional syngas production [6]. However, the process only converts methane, and more importantly, generates a significant amount of CO_2 (approximately, 7 kg CO_2 per 1 kg H_2), contributing to 3% of total greenhouse gas emissions [7]. By contrast, DRM does not produce any CO_2 emissions and efficiently converts greenhouse gases (CH_4 and CO_2) as reactants to produce syngas with a H_2/CO ratio of 1, offering a competitive edge in the synthesis of methanol and high-value-added chemicals via the Fischer–Tropsch process [5,8].

Despite the extensive research conducted in this field, existing catalysts still face challenges such as coke formation and sintering, which lead to catalyst deactivation [5,9]. These issues arise because of the high reaction temperatures required in the DRM process. However, previous studies have suggested potential solutions to overcome these challenges [10–12]. One approach involves using bimetallic catalysts alloyed with metals such as Co, Cu, Fe, Mo, and others, which have shown promise in

* Corresponding authors.
E-mail addresses: Insoo@seoultech.ac.kr (I. Ro), kjh24@yonsei.ac.kr (J. Kim).

https://doi.org/10.1016/j.apcatb.2023.123454
Received 13 July 2023; Received in revised form 26 October 2023; Accepted 30 October 2023
Available online 9 November 2023

Nomenclature

DNN	Deep neural network.
DRM	Dry reforming of methane.
Feature	Input variables that cause output in machine learning models.
GHSV	Gas hourly space velocity (mgmin/ML, the reciprocal of commonly used GHSV unit).
GPR	Gaussian process regression.
IML	Interpretable machine learning.
MCM41	Mobile Composition of Matter No.41.
M_I	Initial machine learning model.
ML	Machine learning.
PDV	Partial dependence value.
RF	Random forest.
RMSE	Root mean square error.
SBA-15	Santa Barbara Amorphous-15.
SHAP	Shapley additive explanation.
SVM	Support vector machine.
T	Temperature (℃).
ZSM5	Zeolite Socony Mobil–5.

facilitating coke removal and improving catalyst stability [12,13]. Furthermore, the selection of suitable catalysts, including semi-metals and alkali metal oxide catalysts, has demonstrated the ability to reduce carbon deposition compared to Ni monometallic catalysts, thereby enhancing catalyst durability [5,14]. Consequently, it is crucial to focus on enhancing catalyst performance using a combinatorial optimization strategy that considers the appropriate components and optimal composition of active metals, promoters, and supports [15].

Recently, the integration of machine learning with catalyst research has gained attention as a means to overcome aforementioned challenges and accelerate the development and discovery of novel catalysts [16–21]. Machine learning, as a subfield of artificial intelligence, has proven effective in numerous chemical engineering studies. By utilizing data, machine learning enables accurate pattern recognition, classification, and prediction, offering valuable insights from complex data while minimizing computational costs [22–28]. This approach efficiently explores a broad parameter space. Previous studies have successfully employed machine learning for DRM catalyst development, predicting key catalyst performance indicators such as CH_4 conversion, CO_2 conversion, syngas ratio, and carbon deposition [29–32]. Outstanding models capable of accurate predictions have been proposed, and variables that have a significant impact on catalyst performance have been analyzed through machine learning models. Additionally, most reported studies have shown satisfactory prediction accuracy with an R^2 value over 0.85 [29–31]. However, certain identified limitations require further research. To apply machine learning methodologies to practical catalyst research, such as proposing and screening promising catalyst candidates, we need to address three main issues: (1) the utilization of highly complex black-box models, (2) catalyst comparison under identical conditions, and (3) examination of diverse combinations of catalysts. This study defines and discusses these three issues in detail.

First, machine learning models are often perceived as black boxes, because comprehending the decision-making process and causal relationships between input and output variables is challenging [32,33]. While domains like image processing or natural language processing allow for intuitive assessment of model predictions, evaluating the performance of materials, such as catalysts, lacks immediate comparability to actual results [16,34]. Consequently, concerns arise regarding the reliability of the model's performance metrics. Some studies have addressed this issue in DRM catalyst performance prediction by analyzing the rationale behind the model's heuristics or decision-making and proposing interpretable model research [29,32,35]. However, the lack of direct validation experiments for these proposed results acts as a barrier, discouraging researchers from implementing such methodologies in practice. In this study, we extensively employed interpretable machine learning (IML) tools to enhance the model's performance and facilitate result analysis, thereby improving the practical reliability of the model. Additionally, we validated the model's predictions not only by comparing them with literature data that were not used for model training but also by conducting direct experimental validation.

Second, the comparison of catalysts under identical conditions is rarely performed [36]. In order to overcome this limitation, we compiled a comprehensive dataset by consolidating individual literature data that were obtained using inconsistent protocols. This approach allows us to offer reliable recommendations and screening capabilities with increased accuracy and consistency [34]. The lack of standardized rules for data collection methods in the context of catalyst data poses challenges in ensuring consistent preprocessing and maintaining uniform reaction condition protocols, except in cases where data are obtained using high-throughput experimental reactors [37,38]. Because of the intricate interactions among multiple variables, including reaction temperature, reduction and calcination temperatures, and the composition and types of active metals, promoters, and supports, the development of effective catalysts becomes increasingly challenging [39]. In this study, we incorporated a separate dataset to systematically test various combinations of catalyst materials under the identical conditions, thereby validating the findings through experimental validation. To the best of our knowledge, in addition to the studies combining DFT, no published reports that use the models directly for recommending or screening promising catalysts exist.

Third, most reported studies have predominantly focused on a narrow selection of metal-based catalysts, primarily Ni and Co, or specific supports such as CeO_2 [12,32]. To overcome this limitation and broaden the scope of exploration, we expanded the model's capabilities to encompass a more diverse range of design variables. This expansion was necessary to prevent the prediction of catalyst performance from being limited to only a few cases [32], thereby aligning with the overarching objective of leveraging machine learning for effective catalyst development. Although this study is also influenced by the abundance of literature data focused on Ni catalysts, we addressed this by incorporating a comprehensive training dataset comprising 22 different active metals and promoters, as well as 24 distinct supports.

In this study, we developed a framework of IML models specifically designed for enhancing the prediction performance of DRM as a model reaction. In the process, we utilized IML tools such as Shapley additive explanations (SHAP) and partial dependence values (PDV), enabling us to gain a comprehensive understanding of the intricate causal relationships and contributions between complex input and output variables involved in the DRM process. Through the utilization of these IML tools, we have gained intuitive insights into the prediction results and obtained insights of the model's decision-making process. Furthermore, we conducted experiments to screen and recommend catalyst candidates by leveraging a meticulously generated dataset, facilitating catalyst comparison under consistent conditions. This direct advice provides valuable assistance to researchers that use machine learning in their decision-making process. Throughout this process, we developed models considering various combinations of catalysts reported in the literature and provided recommendations for catalyst candidates. In addition, we compared the model recommendation results to the results of the experiments performed to ensure the accuracy of our model. The primary objective of this study is to offer a comprehensive model development and analysis process, as well as guidelines for screening potential catalyst candidates. These guidelines are designed to assist researchers involved in the development of catalysts with complex variables.

2. Framework methodology

Fig. 1 shows the overall framework used in this study. The IML framework is mainly composed of four steps: (i) data preparation, (ii) model development, (iii) recommendation of catalyst candidates, and (iv) analysis of model interpretability. In the data preparation step, data collection and preprocessing are performed. In the preprocessing process, feature selection is performed using the Pearson correlation coefficient and SHAP. In the model development step, the best algorithm is selected among various algorithms and the performance of the model is improved through hyperparameter optimization. After development, the performance of the model is evaluated. In the catalyst candidate recommendation step, we use SHAP and PDV to generate a random dataset that reduces the influence of catalyst pretreatment conditions and operating conditions for recommendation, and then use the recommended dataset in the developed model to recommend potential catalyst candidates. Finally, in the model interpretability analysis step, we use PDV to determine the contribution of catalyst material variables to the variation in output values. The PDV enables us to understand the predictive tendencies of the model, as well as gain insights for catalyst design. Furthermore, in the final step, the model is evaluated to ensure that it does not violate existing domain knowledge.

2.1. Dataset preparation

The dataset used in the study was created by combining the data previously reported by Ayes et al. [40] and data collected from other literature [41–63]. The dataset comprised 5655 experimental data points for DRM catalysts from 101 papers published from 2005 to 2014 [29]. More up-to-date data were compiled for this study to develop effective ML model [64]. Therefore, 31 papers published from 2014 to 2021 were added to the original data. Catalysts that were synthesized using special pretreatment or preparation methods were excluded from the dataset. To ensure consistency, the CH_4 conversion with the highest number of instances were extracted from the tables and graphs because yield and selectivity were not consistently reported as output variables. Consequently, the original dataset comprised 6067 datapoints from a total of 132 papers [41–63,65–173] (details are available in Table S1 and Table S2).

The raw dataset comprised 85 variables, including 65 design variables, 12 pretreatment conditions, and eight operating conditions. Ten variables were removed based on the SHAP analysis results during the data preparation step. Before executing the SHAP analysis, we conducted Pearson's correlation analysis to check the suitability of our dataset for SHAP analysis. The results of the Pearson correlation coefficient analysis of our dataset are shown in Fig. S1. Generally, a Pearson correlation coefficient with an absolute value of 0.3 or higher indicates a weak linear relationship, whereas a coefficient of 0.7 or higher suggests a strong correlation [174]. The Pearson correlation coefficient between the operating variables, CH_4 and CO_2 proportion ratio in the reactant gas, reaction temperature, and ratio of reactant gas, was 0.5 or greater, suggesting a significant correlation with conversion. Because the operating variable will be used as data generated by manipulation, except for the reaction temperature, the dataset appeared suitable for SHAP. After preprocessing, the dataset was modified to fit our model with 5655 data points with 65 variables. A detailed list of variables for the original and modified datasets is presented in Table S1 and Table S2. The modified dataset is shown in Table 1.

2.2. Interpretable machine learning tools

To facilitate the preprocessing of the model's dataset, interpretation

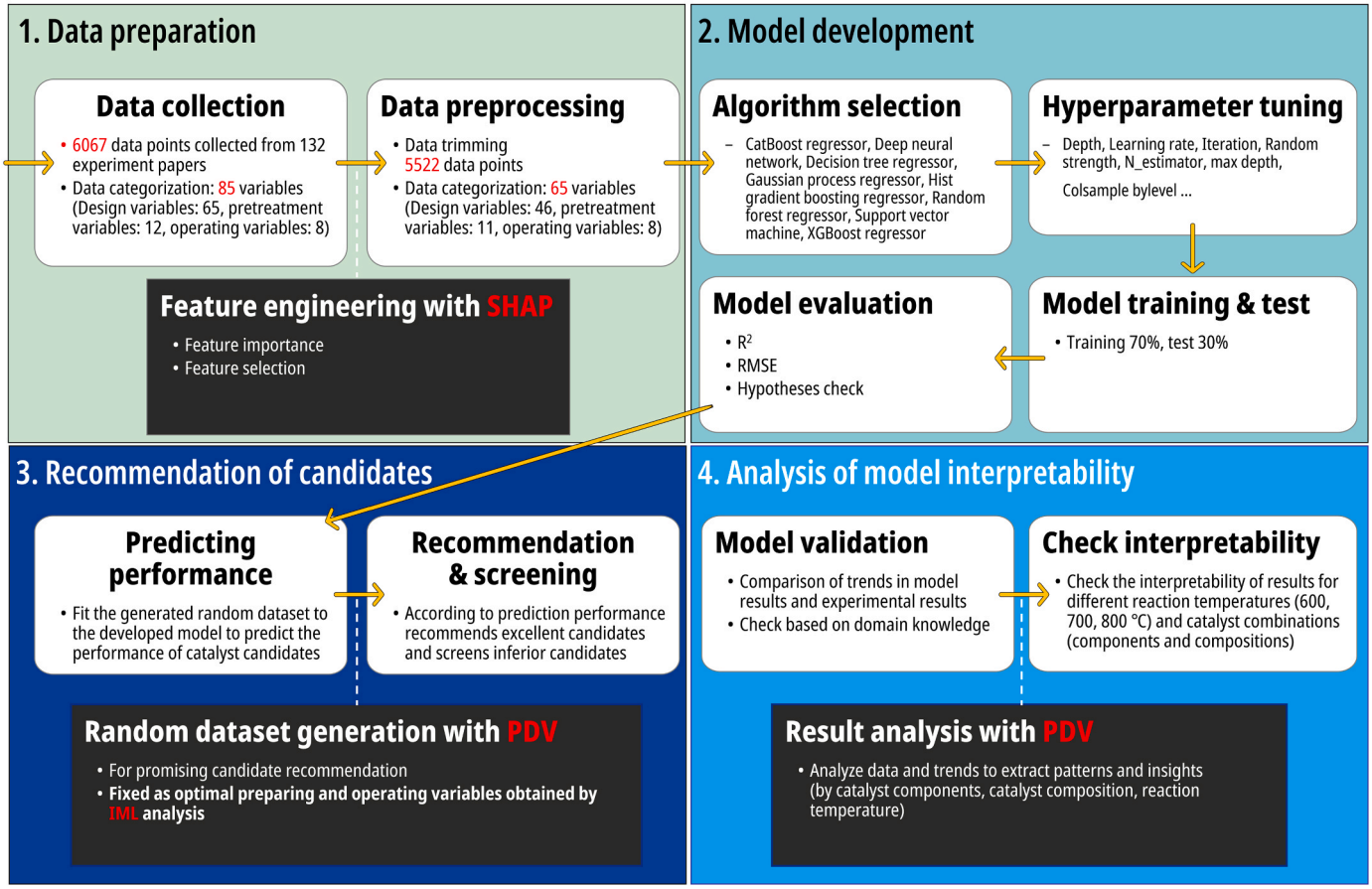

Fig. 1. Overall framework to develop a model for a catalyst.

Table 1
Element and its maximum value for each variable in the modified dataset.

Input variables		Ranges for continuous or identities for discrete variables					
Design variables	Active metal of catalyst (wt%)	Element	Maximum	Element	Maximum	Element	Maximum
		Au	0.20	Mn	5.00	Rh	7.25
		Co	30.00	Ni	30.00	Ru	5.00
		Cu	11.00	Pd	5.00		
		Ir	5.00	Pt	5.00		
	Promoter of catalyst (wt%)	Element	Maximum	Element	Maximum	Element	Maximum
		Ba	2.69	K	5.00	Sr	2.25
		Ca	5.00	La	14.45	Y	9.00
		Ce	15.00	Li	0.50	Pr	5.00
		Fe	5.10	Mg	8.00	Zr	11.11
	Support of catalyst (wt%)	Element		Maximum	Element		Maximum
		Al_2O_3(Alpha)		100	MgO		100
		Al_2O_3(Gamma)		100	MnO		15
		Al_2O_3(Mesoporous)		100	PrO_2		20
		BaO		100	SBA15		100
		BN		100	Si_3N_4		100
		CaO		49	SiO_2		100
		CeO_2		100	TiO_2		100
		La_2O_3		100	V_2O_5		10
		MCM41		100	Y_2O_3		20
		$MgAlO_4$ (Nanocrystalline)		100	ZrO_2 (Nanocrystalline)		100
		$MgAlO_4$		100	ZrO_2		100
		MgO (Nanocrystalline)		100	ZSM5		100
Pretreatment variables	Pretreatment Methods	Co-impregnation (CI), Co-precipitation (CP), Incipient to wetness impregnation (IW), Sol-gel method (SG), Sequential impregnation (SI), Wet impregnation (WI)					
	Maximum and minimum values for each pretreatment variable	Variable				Minimum	Maximum
		Calcination Temperature (℃)				300.00	930.00
		Calcination Time (hour)				0.50	15.00
		Reduction Temperature (℃)				0.00	1000.00
		Reduction Time (hour)				0.00	24.00
		Proportion of H_2 in the reduction gas (vol%)				0.00	100.00
Operating variables	Maximum and minimum values for each pretreatment variable	Variable				Minimum	Maximum
		Reaction Temperature (℃)				350.00	900.00
		Proportion of CH_4 in the reactants (vol%)				7.00	83.33
		Proportion of CO_2 in the reactants (vol%)				7.00	83.33
		Proportion of Ar in the reactants (vol%)				0.00	81.80
		Proportion of N_2 in the reactants (vol%)				0.00	80.00
		Proportion of He in the reactants (vol%)				0.00	86.00
		Gas hourly space velocity of catalyst (mgmin/ML)				0.001	88.24
		Reaction time (min)				Initial time	7800.00

of recommendation results, and evaluation of the model, we appropriately utilized IML tools. The IML tools used in this study include SHAP and PDV. We implemented SHAP plots using the SHAP software library, whereas PDV values were computed and visualized using the functionality provided by the scikit-learn library. SHAP employs a fair allocation method based on cooperative game theory to determine the rank and contribution of each variable's impact on the model. It enables the interpretation and inference of comprehensive and intuitive variables as well as results. Similarly, PDV, which is model-agnostic, tests the marginal effects of input variables on the predicted target outcomes of the trained machine learning model. It assists in the comprehensive and intuitive inference and interpretation of variables and results. Detailed theoretical backgrounds and computational results for SHAP and PDV are provided in supplementary material S3 and Fig. S2.

2.3. Model development and performance evaluation

All modeling and calculations were performed using the open-source software Python. The dataset was confirmed to be sufficiently independent through cross-validation. Cross-validation results are provided in supplementary material Fig. S3. For faster computation speed in making predictions, the dataset was split using the holdout method, where it was randomly divided into training data for model training (70%) and test data for model performance evaluation and validation (30%) [29,175–178].

2.3.1. Model algorithm selection

In this work, eight algorithms were compared for modeling: CatBoost regressor, decision tree regressor, deep neural network, Gaussian process regressor, Hist gradient boosting regressor, random forest regressor, support vector machine, and XGBoost regressor. In the cases wherein deep neural networks, Gaussian processes, and support vector machine algorithms were used, the dataset was standardized with the standard scaler of the scikit-learn library. As shown in Fig. S4, when the hyperparameters are fixed as default values, the tree-based models exhibit high accuracy. The CatBoost algorithm exhibited the highest prediction accuracy with an r-squared (R^2) of 0.96 and root mean square error (RMSE) of 5.2663, which is in agreement with previous studies [179].

CatBoost has a simpler hyperparameter optimization process than other algorithms, such as neural networks; it has a shorter model learning time and can interpret the driving principle of the model. Therefore, CatBoost was chosen for this study. CatBoost is an open-source algorithm developed by Prokhorenkova et al. [180] to provide exceptional performance based on categorical variables by adding gradient boosting to a general decision tree model. In contrast to the existing gradient boosting decision tree algorithm, permutations are obtained by randomly calculating the average label value of a dataset with the same categorical value as a given value, rather than approximating and calculating all permutations [179]. This shortens the required calculation time. The decision tree function of CatBoost is calculated using Eq. (1) [180]:

$$h(x) = \sum_{j=1}^{J} b_j 1_{\{x \in R_j\}}, \quad (1)$$

where h(x) is a decision tree function of an explanatory variable x and $R_j$is the disjoint region corresponding to the leaves of tree.

2.3.2. Hyperparameter optimization

CatBoost has various hyperparameters that improve model performance [181]. In this study, the hyperparameters of CatBoost were tuned using the grid search method. The accuracy of the model for individual hyperparameters is shown in Fig. S5. in the supplementary material. The accuracy of the model was compared by dividing it into a training and test dataset. A model is considered to be overfitted if the test accuracy is higher than that of the training data [182]. The types and values of the CatBoost hyperparameters are as follows: 1000 iterations were used and the learning rate was 0.09, depth was seven, eval metric was RMSE, bagging temperature was one, od type was 'Iter,' metric period was 75, and od wait was 100.

2.3.3. Model evaluation

This study used R^2 and RMSE as evaluation criteria to evaluate the accuracy and predictive performance of the model. R^2 and RMSE were calculated using Eqs. (2) and (3) [183]:

$$R^2 = 1 - \frac{\sum_{k=1}^{N}(S_{ka} - S_{kp})^2}{\sum_{k=1}^{N}(S_{ka} - \overline{S}_{ka})^2}, \quad (2)$$

$$RMSE = \sqrt{\frac{\sum_{k=1}^{N}(S_{ka} - S_{kp})^2}{N}} \quad (3)$$

where N is the number of data points, S_{ka} is k^{th} real value, S_{kp} is k^{th} predicted value, and $\overline{S}_{ka}$is average value of S_{ka}.

2.4. Recommendation of potential DRM catalyst candidates

In DRM, similar to other thermal catalytic reactions, the reaction temperature has been identified as the dominant variable for conversion [143]. However, the SHAP results depicted in Fig. 2(a) and S6 reveal that more than 10 features related to preprocessing and tasks have a significant impact on the conversion among the top 20 contributing features. Hence, to obtain model results that consider the influence of design variables, catalysts must be screened using a dataset wherein both the pretreatment and reaction conditions are maintained constant.

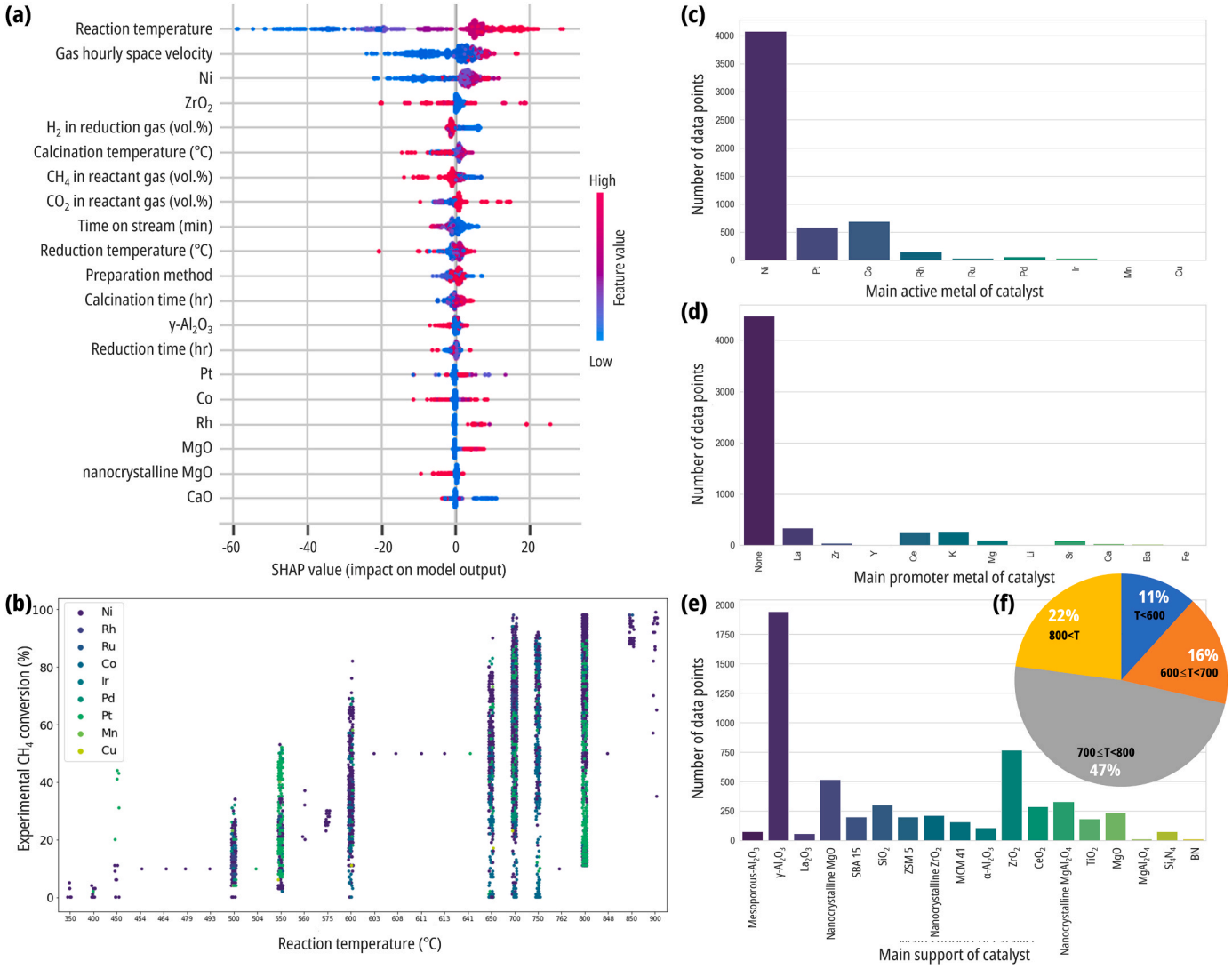

Fig. 2. Data analysis of original dataset: (a) top 20 variables with feature importance, (b) reaction temperature and experimental CH_4 conversion by major active metal, (c) number of data points by active metal, (d) number of data points by promoter, (e) number of data points by support, and (f) distribution of data points by reaction temperature.

To identify potential catalyst candidates worth experimental verification, we present in Table 2. Furthermore, the dataset was constructed by prioritizing preprocessing and reaction conditions as detailed in Section 6. Moreover, to create various combinations that alter the catalyst's components and composition, a dataset comprising 1 million combinations was generated using the random module in Python. By analyzing the existing literature data and utilizing the generated data and models, similar to the concept of high-throughput devices, predicted results can be obtained under controlled conditions, providing output values for design variables and reaction temperatures [34,184].

3. Experimental section

3.1. Preparation of catalysts

The catalysts were prepared using the incipient wetness impregnation method, wherein an appropriate amount of active metal precursor was dissolved in deionized (DI) water and stirred at room temperature for 10 min. The supports used in this study were γ-Al_2O_3, SiO_2, and ZSM5 (SiAl = 50). γ-Al_2O_3, MgO, SiO_2, and ZrO_2 were purchased from Sigma Aldrich, whereas ZSM5 was purchased from Alfa Aesar. The support was dried at 100 ℃ for 6 h before impregnation. The used active metal and promoter precursors were purchased from various suppliers and used without further customization. $Ca(NO_3)_2$•4 H_2O, $Ce(NO_3)_3$•6 H_2O, $Cu(NO_3)_2$•3 H_2O, and $Fe(NO_3)_3$•9 H_2O were purchased from ACROS Organics. $Y(NO_3)_3$•6 H_2O and $RuCl_3$•xH_2O were purchased from Alfa Aesar. $La(NO_3)_3$•6 H_2O was purchased from Thermo fisher. KNO_3, $Mg(NO_3)_2$•6 H_2O, $Ni(NO_3)_2$•6 H_2O, $PdCl_2$, $Pr(NO_3)_3$, and $Pt(NH_3)_4$•$(NO_3)_2$ were purchased from Sigma Aldrich. After the impregnation procedure, the catalysts were dried at 100 ℃ for 1 h and calcined at 800 ℃ for 2 h with a heating rate of 5 ℃/min, under a 100 ML/min flow of an air. Table 2 lists prepared catalysts for the validation experiments. In the case of promoting support and support, the total sum was set to 100%, and the loading of active metal and promoter indicates the corresponding percentages with respect to this 100% support.

3.2. Catalytic test

An experimental setup for the DRM reaction was created as described in [185]. The DRM activity of the catalyst was measured using a tubular quartz fixed bed reactor at atmospheric pressure. The quartz tube has a length of 600 mm divided into two sections (300 mm + 300 mm) with different diameters. The upper section has inner and outer diameter of 10 mm and 12 mm, respectively, and the lower section has inner and outer diameter of 7 mm and 9 mm, respectively. The dry reforming reaction was initiated by introducing a gas mixture of reactants. 20 mg of the catalyst was diluted with 200 mg of silicon carbide and placed in the middle of the tube packed with quartz wool.

Prior to experimental test, the catalyst sample were reduced for 2 h with a heating rate of 5 ℃/min, under 50% H_2/Ar mixture (100 ML/min) at 800 ℃. After the reduction, the catalyst bed was then purged with pure N_2 (20 ML/min) for 15 min to remove all remaining hydrogen. The catalysts were tested for 5 h with a heating rate of 25 ℃/min, under CH_4:CO_2:N_2 mixture gas with a volume ratio of 45:45:10 (100 ML/min) at 800 ℃. The gas product was analyzed using a gas chromatograph (GC) – thermal conductivity detector equipped with a Carboxen-1000 column. The conversion of CH_4 was calculated using the following Eq. (4):

$$CH_4 \quad conversion(\%) = \frac{F(CH_4, in) - F(CH_4, out)}{F(CH_4, in)} \times 100 \tag{4}$$

4. Results and discussion

4.1. Result of data analysis and preparation with SHAP

The contribution of each feature in the original dataset was analyzed using SHAP to demonstrate the effectiveness of SHAP as an IML tool.

The original dataset can be visually analyzed as in Fig. 2. Fig. 2(a) shows a comparison of the features contributing the most to the model's predictions using SHAP. Among thermal catalytic reactions, in the case of endothermic reactions such as DRM reactions, the effect of reaction temperature has the greatest influence on the performance of the catalyst [120,186]. Therefore, as shown in Fig. 2(f), we can observe that data points for reaction temperatures between 700 °C and 800 °C were collected with the highest frequency, approximately 47% of the data set. According to the SHAP value in Fig. 2(a), the feature that contributes the second most to the prediction is gas hourly space velocity. This result is consistent with the existing domain knowledge that the gas hourly space velocity of the catalyst, which is determined by the flux and amount of the total catalyst loaded in the reactor, significantly contributes to the conversion. Ni is the third most contributing variable because Ni is an active metal, which has been widely used in the past owing to its low price and high availability. However, further development is required for DRM catalysts using Ni because of issues related to carbon formation and sintering of metals [42,45,143]. Fig. 2(b) shows the change of reaction temperature and conversion for active metal. Although reaction temperature and conversion appear to be highly correlated, high

Table 2
Cases of catalysts impregnated for the validation experiments of the screening.

Catalyst No.	Catalyst case	Active metal		Promoter		Promoting support		Support	
		Component	**Loading (wt %)**	**Component**	**Loading (wt %)**	**Component**	**Loading (wt %)**	**Component**	**Loading (wt %)**
1	**Ni(5)/** γAl_2O_3	**Ni**	**5**					γAl_2O_3	**100**
2	Ni(5)-Y(5)/γAl_2O_3	Ni	5	Y	5	-	-	γ-Al_2O_3	100
3	Ni(5)/Pr_xO_y-γAl_2O_3	Ni	5	-		Pr_xO_y	5	γ-Al_2O_3	95
4	Ni(3)-Y(2)/Pr_xO_y-γAl_2O_3	Ni	3	Y	2	Pr_xO_y	5	γ-Al_2O_3	95
5	Ni(3)-La(2)/Pr_xO_y-γAl_2O_3	Ni	3	La	2	Pr_xO_y	5	γ-Al_2O_3	95
6	Ni(3)-Ca(2)/Pr_xO_y-γAl_2O_3	Ni	3	Ca	2	Pr_xO_y	5	γ-Al_2O_3	95
7	Ru(3)-Y(2)/Pr_xO_y-γAl_2O_3	Ru	3	Y	2	Pr_xO_y	5	γ-Al_2O_3	95
8	Ce(3)-Ni(2)/Pr_xO_y-γAl_2O_3	Ce	3	Ni	2	Pr_xO_y	5	γ-Al_2O_3	95
9	Ni(3)-Pd(2)/Pr_xO_y-γAl_2O_3	Ni	3	Pd	2	Pr_xO_y	5	γ-Al_2O_3	95
10	Ni(3)-Cu(2)/CaO-γAl_2O_3	Ni	3	Cu	2	CaO	5	γ-Al_2O_3	95
11	Ni(3)-Mg(2)/CaO-γAl_2O_3	Ni	3	Mg	2	CaO	5	γ-Al_2O_3	95
12	Ni(3)-Fe(2)/CaO-γAl_2O_3	Ni	3	Fe	2	CaO	5	γ-Al_2O_3	95
13	Ni(3)-Pr(2)/CaO-γAl_2O_3	Ni	3	Pr	2	CaO	5	γ-Al_2O_3	95
14	Ni(3)-La(2)/Pr_xO_y-ZSM5	Ni	3	La	2	Pr_xO_y	5	ZSM5	95
15	Ni(5)/Y_xOy-SiO_2	Ni	5	-	-	Y_xO_y	5	SiO_2	95
16	Ce(5)/YxOy-SiO_2	Ce	5	-	-	Y_xO_y	5	SiO_2	95
17	Fe(5)-Y(5)/SiO_2	Fe	5	Y	5	-	-	SiO_2	100

temperature does not always directly correlate with high conversion values.

An intriguing finding in the data analysis results is the pronounced prevalence of certain active metals, promotors, and supports, as depicted in Fig. 2(c-e). Notably, Ni, Co, and Pt stand out as the most commonly utilized metals, comprising a significant 95% of the total data points. These metals hold significant importance among the design variables within the original dataset. Consequently, the SHAP analysis indirectly suggests that data collection should focus on active metals other than Ni, Pt, and Co to reduce model bias. In addition, the rankings of SHAP values for supports and the frequencies of data are consistent. By contrast, the SHAP value for promoters is relatively low compared to supports and active metals. This observation can be interpreted as the promoter having a lower impact on DRM activity compared to the active metal and support. However, we attribute this to the limited frequency of data points that include the promoter. Therefore, proposing an effective combination considering various promoters using a machine learning model could be beneficial for the development of DRM catalysts. In Fig. S6, the SHAP values for each reaction temperature are compared by dividing them into four sections: less than 600 ℃, between 600 ℃ and 700 ℃, between 700 ℃ and 800 ℃, and greater than 800 ℃. As shown in Figs. S6 (a) and (b), for reaction temperatures less than 700 ℃, the reaction temperature has the highest SHAP value, indicating its significance as the most important feature. However, for reaction temperatures greater than 700 °C, the gas hourly space velocity (GHSV) becomes more important. This is because high temperatures do not necessarily guarantee higher conversion; however, if the reaction temperature increases beyond a certain point, the conversion is significantly influenced by the reaction rate, such as when the catalyst does not have sufficient reaction time or when the contact time is excessively long [9]. From a component perspective, it is noteworthy that the effect of ZrO_2, including the nanocrystalline structure, varies with each reaction temperature. In the relatively low temperature range from less than 600 ℃ to between 600 ℃ and 700 ℃, an increase in the value of ZrO_2 positively contributes to the increase in CH_4 conversion. However, in the range of 700 ℃ or greater, the pattern is reversed. Fig. S6(c) shows that the SHAP values of the ZrO_2 nanocrystalline structure exhibit a negative correlation, and Fig. S6(d) demonstrates that ZrO_2 has the highest SHAP value and that CH_4 conversion decreases with increasing ZrO_2 value. Moreover, for reaction temperatures greater than 800 °C, six variables correspond to the support, emphasizing the importance of selecting an appropriate support to maintain catalyst reactivity, particularly at high temperatures [5].

The effect of synergies among design variables that compose the catalyst combination and the dominant variable, reaction temperature, on the final conversion is shown in Fig. 3(a) as an alluvial plot. By dividing the conversion results into quartiles based on the conversion values in the entire original dataset, Fig. 3(a) shows that Q1, which includes conversion results ranging from 78% to 98%, requires a reaction temperature of 700 ℃ or higher. In general, as the reaction temperature decreases, the CH_4 conversion tends to decrease. Notably, some combinations belong to the category of Q4, low conversion results can range from 0% to 34% even at high reaction temperatures of greater than 800 ℃.

We further analyze the results presented in Fig. 3(b-d) by color-coding them based on the active metal and promoting support. As shown in Fig. 3(b), in we can observe that Pt and Rh metals are extensively used at relatively low temperatures of 500 °C and 550 °C during the conversion by active metal. This can be attributed to the research focus on developing catalysts with high conversion even at reduced reaction temperatures by utilizing noble metals. In Fig. 3(b), Ni was employed with various supports and promoting supports. In the case of

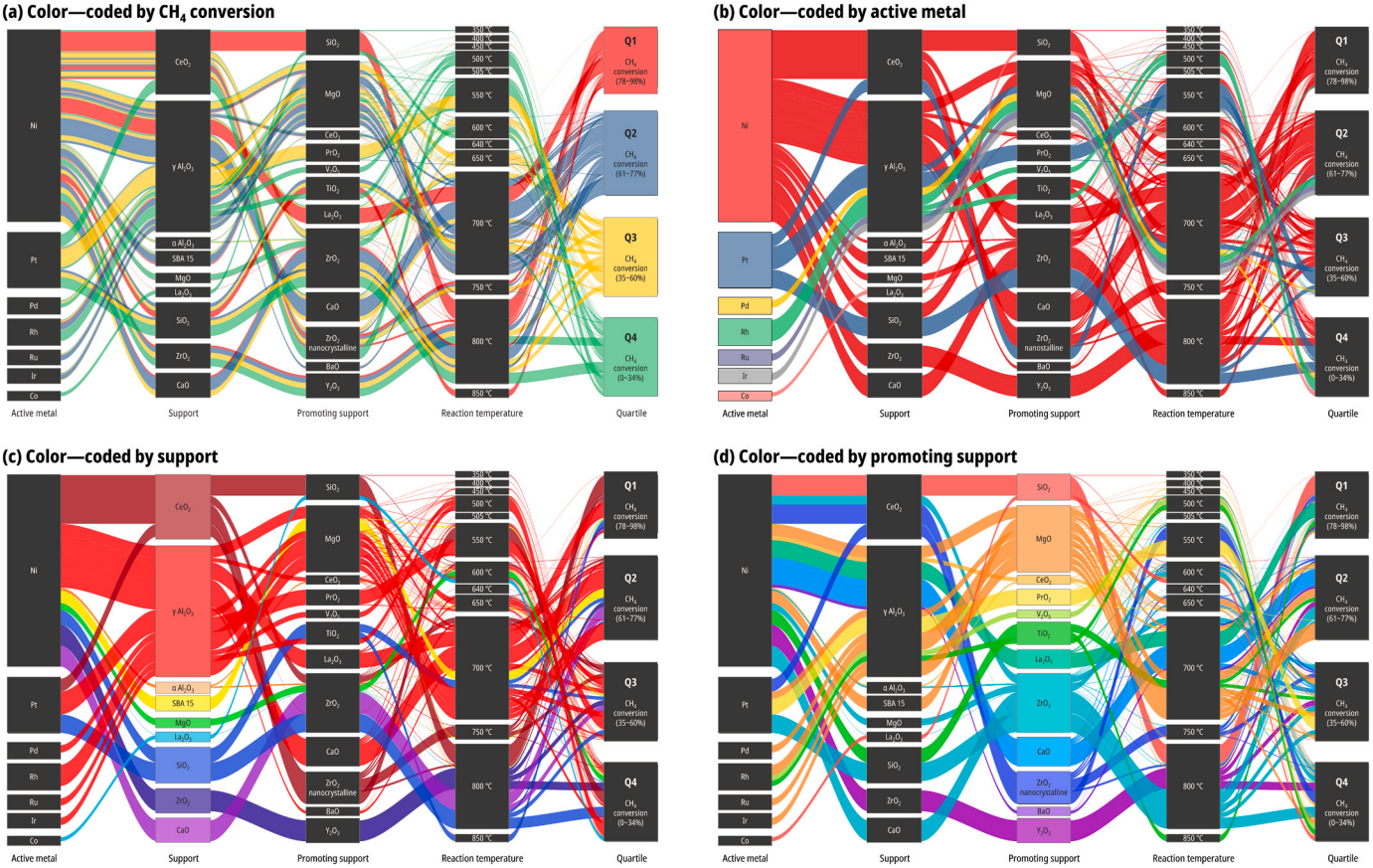

Fig. 3. Comparison of CH_4 conversion by color coding: (a) group of CH_4 conversion, (b) active metal, (c) support, and (d) promoting support.

Pd, it reacted at 700 °C in combination with γAl_2O_3 and MgO, but achieved relatively low conversions in Q3 and Q4, indicating that it is not a particularly noteworthy active metal. Conversely, Ru and Ir, similar to Pd, exhibited conversions equivalent to Q2 when combined with γAl_2O_3 and MgO, demonstrating their potential as active metals worthy of further research and experimentation. Finally, Co, proposed as a replacement for the commonly used Ni, displayed relatively low conversion because it reacted at a temperature of 600 °C. In Fig. 3(c), we color-coded the supports, and it is worth noting that CeO_2 and SBA15 exhibited superior performance for their conversion results corresponding to Q1 and Q2, despite being used relatively infrequently. In addition, the challenges in obtaining intuitive considerations from Figs. 3(c) and 3(d) suggest that the proposed IML framework and the interpretation of results are beneficial for the catalyst development process.

Fig. 4 and Table S1 provide a detailed comparison of the predictive accuracy between the model using the original dataset and the model using the modified dataset based on SHAP and Pearson correlation analysis. The modified dataset, obtained by reducing the number of data points (6067→5655) and eliminating 23 related variables, resulted in improved R^2 and RMSE values of the model, from 0.9077 to 0.9601 and from 7.5246 to 4.9411, respectively. This indicates an enhancement in the accuracy and precision of the model. The improved performance can be attributed to the modification of the dataset, which incorporated the SHAP values as an IML tool. By eliminating variables with minimal contributions to the prediction results, we addressed the issue of unnecessarily large dimensions in the model. Additionally, the reduction of outliers and confounding variables further improved the model's predictive performance. Hence, PDV as an IML technique has the potential to actively enhance the performance of machine learning models through feature and outcome analysis [179].

4.2. PDV of pretreatment and operating variables for dataset generation

As described in Section 2.4.1, the proposed framework was executed to reduce the contribution of the pretreatment and operating variables to the prediction results. The effect of other variables, except the dominant reaction temperature, was also analyzed. Fig. 5 shows the PDVs for the pretreatment and operating variables of the DRM reaction for a fixed reaction temperature. These self-sufficient results provide a plausible insight for the catalytic development of DRM reactions. Fig. 5(a) shows an optimal calcination pretreatment condition (temperature of approximately 500–650 °C and duration of approximately 6–12 h) with a high PDV according to the calcination temperature and time. Fig. 5(b) shows an optimal reduction pretreatment condition (temperature of approximately 700–800 ℃ and duration approximately of 2–4 h). These are not the reaction conditions that guarantee the best performance for catalysts for all the aforementioned DRM reactions; therefore, they may not be directly applicable, but they provide a range of conditions that are worth testing for researchers seeking to experiment with DRM reactions. Fig. 5(c) shows the PDVs according to each composition of CO_2 and CH_4 in the reactant gas. A CO_2/CH_4 of approximately 2–2.5 was shown to be advantageous for a DRM reaction. Fig. 5(d) indicates that the PDV is at a maximum in wet impregnation; however, the difference between the maximum and minimum values is relatively small (0.7). This represents a difference of less than 10% in terms of conversion, and the data are not anticipated to show a significant difference in the resulting conversion because of limitations in the synthesis possibilities based on the components and composition of the catalysts. Fig. 5(e) illustrates the potential influence of both carrier gas type and the proportion of reactant gas on the PDV values. While there is a visually noticeable difference for Ar at 80 vol%, it is important to note that the disparity in PDV value between the maximum and minimum values is only four, rendering it insignificant. Fig. 5(f) shows that as the GHSV increased, the PDV steeply climbed from 38 to 65 with a slight fluctuation, and at the point where the GHSV was 20 or more, the PDV leveled off at 63. Fig. 5(g) shows that the PDV declined as the stream time elapsed from the initial value to 200 min, and converged to nearly 53 after 200 min. Furthermore, Fig. 5(g) shows that the absolute difference value of the PDV does not change markedly by approximately five. Hence, the utilization of PDV has been confirmed to be advantageous in facilitating the selection of priorities and optimal conditions by intuitively analyzing the contribution of the conversion.

4.3. Result of model interpretability

Fig. 6 presents a comparison of the PDV for the active metals and promoters as a function of temperature. Fig. 7 also demonstrates similar trends when comparing conversions by component, but the results depicted in Fig. 6 are more readily interpretable. In the case of Co, Ni, Rh, Ca, and Y, these components have a positive effect on the PDV, even with certain fluctuations. This indicates that the model assesses these

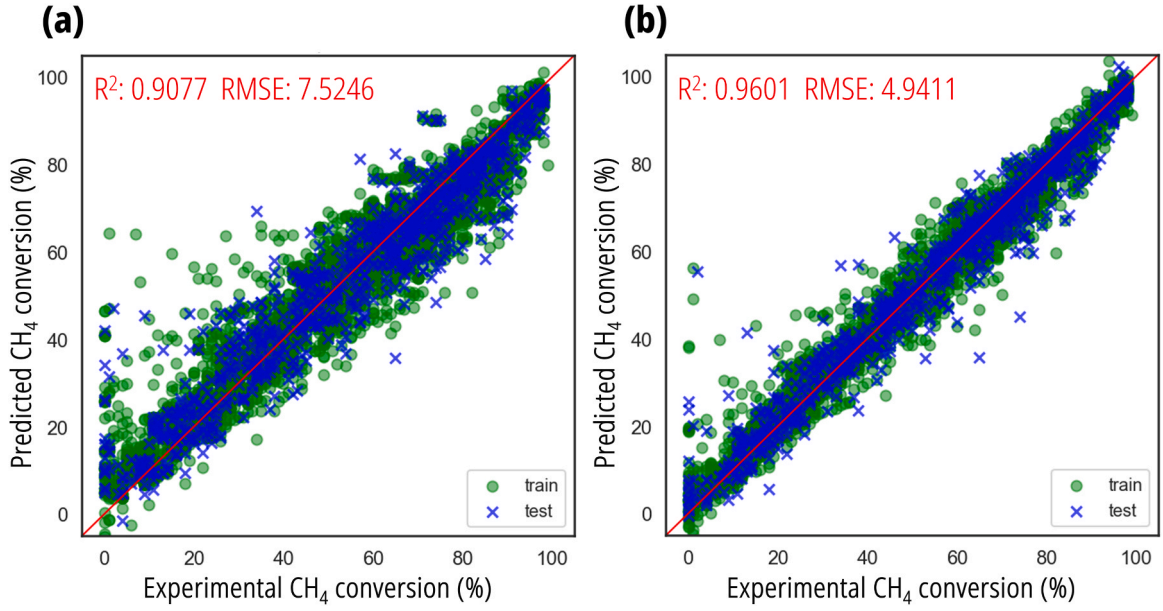

Fig. 4. Comparison of CH_4 conversion prediction accuracy: (a) original dataset and (b) modified dataset after using SHAP.

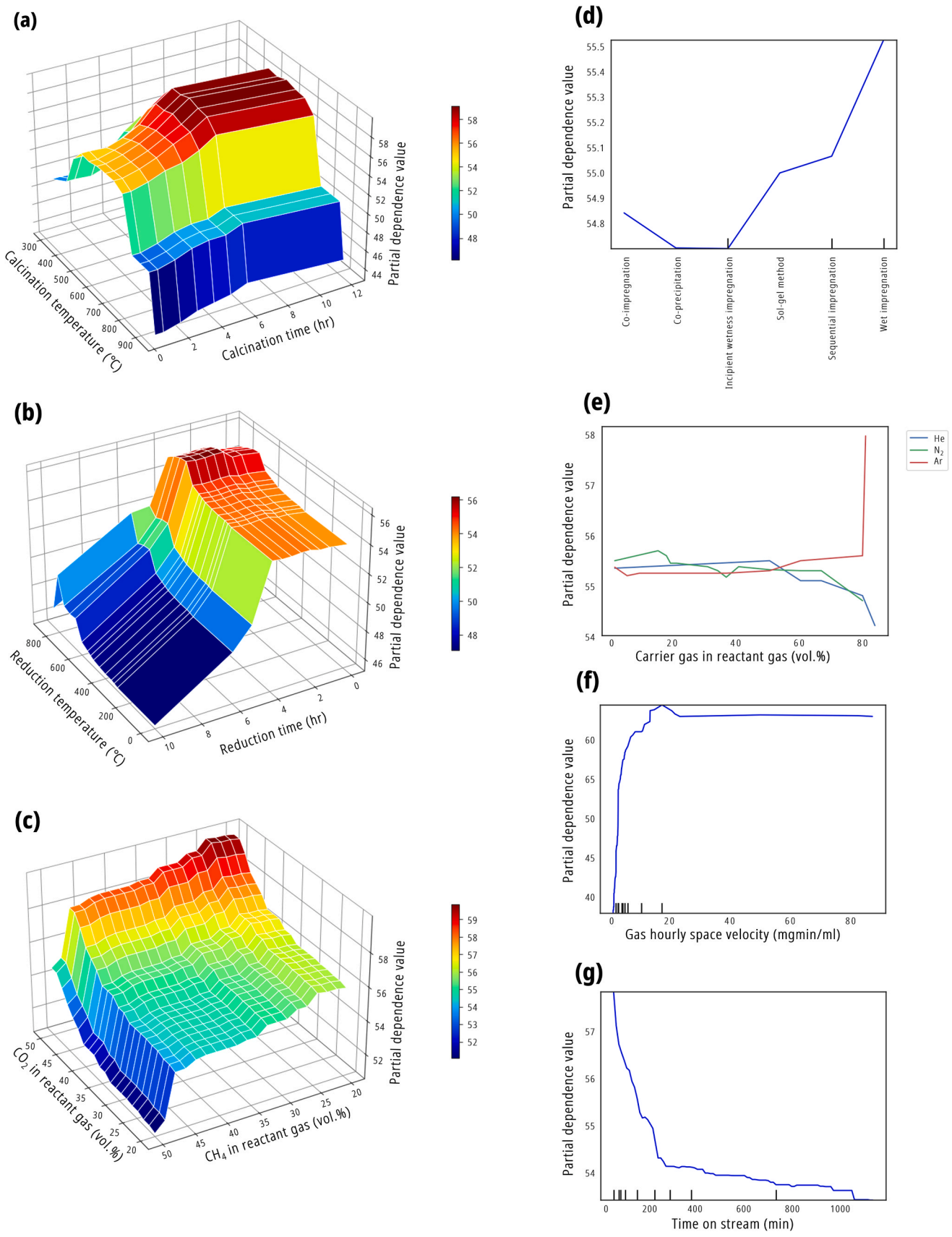

Fig. 5. PDV by operating and pretreatment variables: (a) calcination temperature and calcination time, (b) reduction temperature and time, (c) CO_2 and CH_4 proportion in reactant gas, (d) pretreatment methods, (e) carrier gas type and proportion in reactant gas, (f) GHSV, and (g) time on stream.

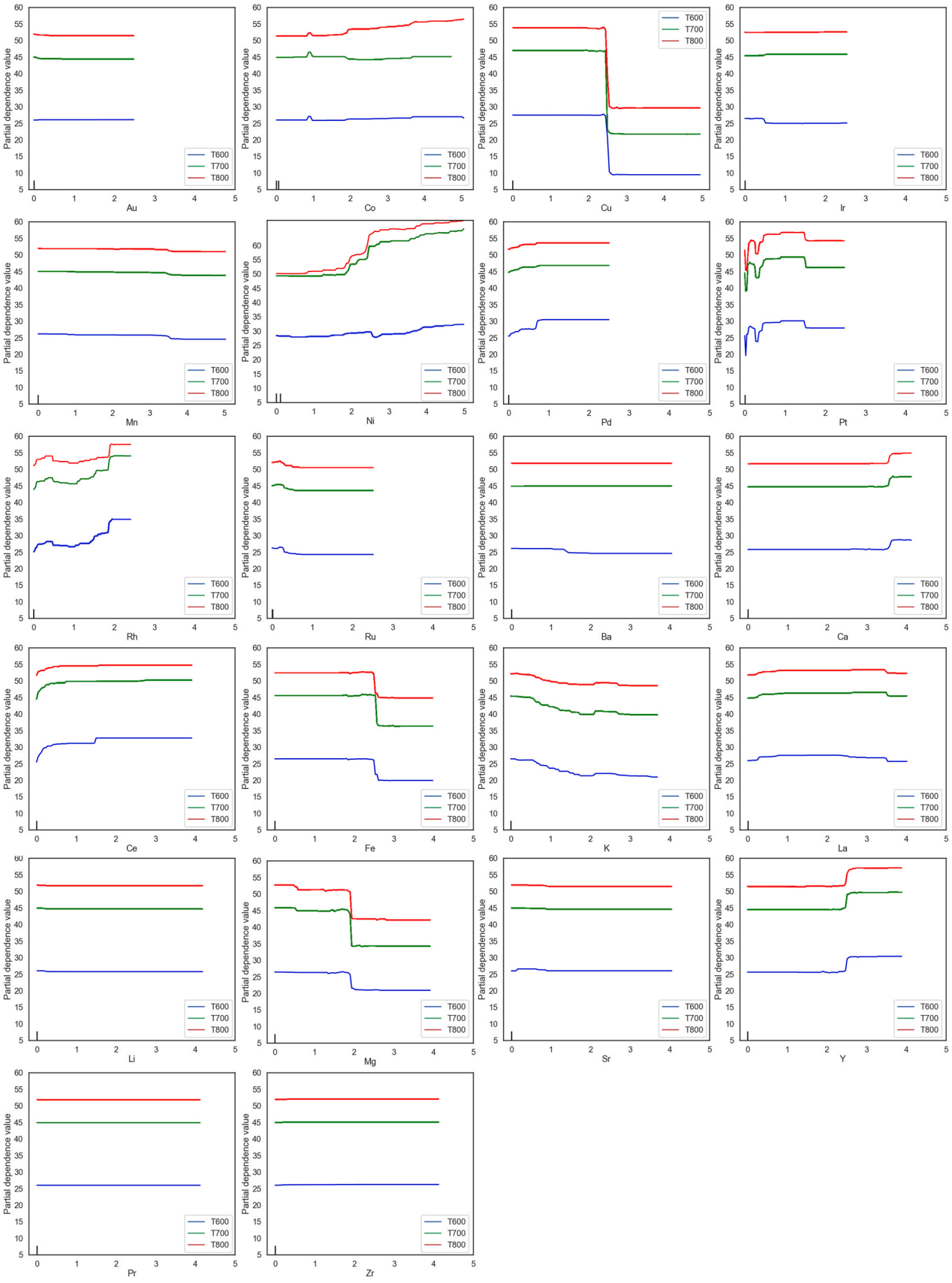

Fig. 6. Comparison of PDV by reaction temperature and component.

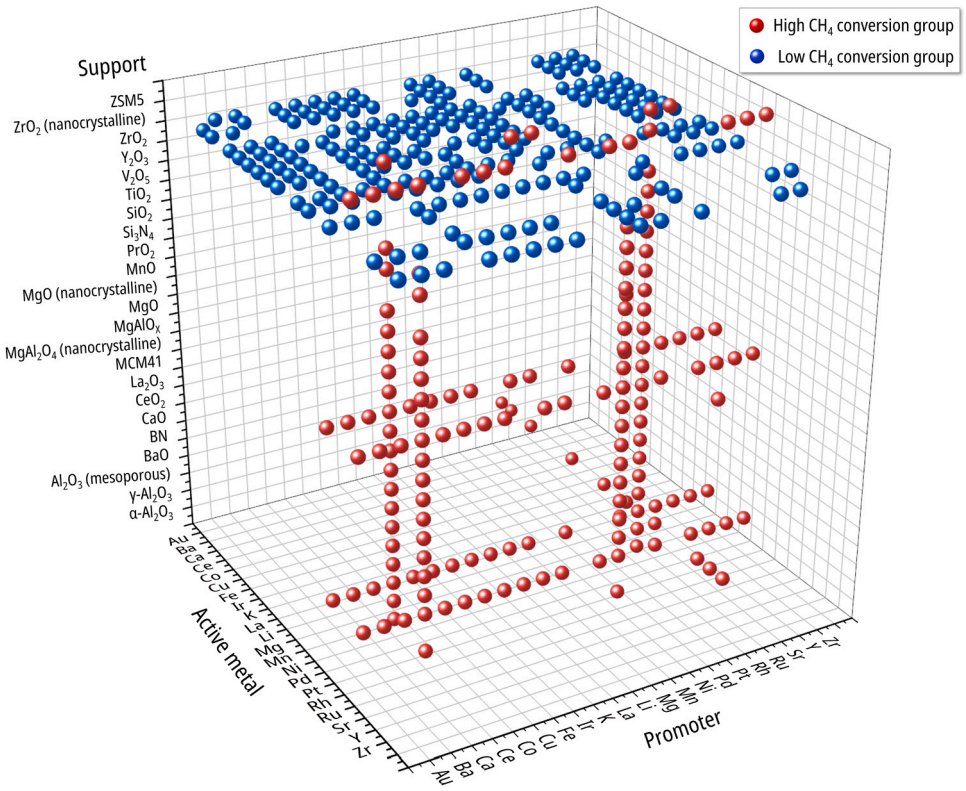

Fig. 7. Scatter plot for comparing the combination of the high and low conversion group.

components as having the potential to result in high conversion, particularly when used with increased loading. By contrast, Cu, Fe, K, and Mg show significant negative effects. This suggests that these components may not be suitable as catalysts for DRM reactions. However, it is noteworthy that the negative effects may be attributed to the model excluding combinations that, according to its assessment, could have led to good conversions. Considering the PDV used in our study, it is important to be cautious in the interpretation of the results. Although the availability of data points enables us to infer the contributions within the observed range, hidden areas may exist without data that could lead to over- or under-interpretation. Nonetheless, the PDV analysis helps researchers make informed choices by identifying suitable components and trends within the loading range. We propose that PDV can be utilized as an indirect tool to assist in selecting the appropriate elements for DRM catalysts.

Fig. 7 shows a scatter plot illustrating the results obtained from the combination of active metal, promoter, and support while dividing the results into a high CH_4 conversion group (top 1%) and a low CH_4 conversion group (bottom 1%) at the reaction of temperature of 800 °C, with the active metal fixed at 3 wt% and the promoter fixed at 2 wt%. These results were obtained from generated data assuming a time on stream of 30 min and maintaining all the preprocessing and operating variables mentioned as the main contributions in this manuscript same. As illustrated in Fig. 7, the plot reveals the importance of active metal and promoter selection for the group with higher conversion results. When Ni and Rh are used as active metals or promoters, we can observe that points from a high group are concentrated. However, even when visualizing selected subsets of data in the simplest graph form, as shown in Fig. 6, we can observe that insights through PDV can provide researchers with valuable information more quickly. This observation aligns with previous studies indicating that ZrO_2, as an oxide support, exhibits relatively low conversion during the initial stages of the reaction, with a time on stream (TOS) of 30 min. Notably, although it is not covered in this manuscript, ZrO_2 has been reported to enhance coke resistance by facilitating CO_2 dissociation on its surface because of its high oxygen mobility. Hence, ZrO_2 could yield better results compared to other supports after a prolonged reaction time surpassing the TOS of 30 min.

4.4. Results of potential DRM catalyst candidates

The heatmap is obtained by predicting the CH_4 conversion while maintaining the support as well as preprocessing and operating variables fixed. For the active metal and promoter components, we depict results in Fig. 8 for the case in which we limited the total loading to 5% by weight to prevent overly optimistic conversion rates as predicted by the model. Following literature reports, while generating the data, the active metal was fixed at 3 wt% and the promoter at 2 wt%. The support, γ-Al_2O_3, was chosen because it is frequently mentioned in the literature and reportedly exhibit high activity in both monometallic and bimetallic catalysts. The performance was predicted using γ-Al_2O_3 as the support. The predicted results indicated that the Rh-Ce and Rh-Pd catalysts exhibited the highest predicted CH_4 conversion at reaction temperatures of 600 °C and 700 °C, respectively. However, at 800 °C, the Ni-Rh catalyst exhibited the highest predicted CH_4 conversion. Considering the cost of catalysts for commercializing DRM reactions, components such as Ce and Y, excluding precious metals (Au, Ir, Pd, Pt, and Rh), are more worth considering for experimental attempts. Furthermore, contrary to previous reports that highlight the positive effects of metal particle dispersion and electronic structure changes in Cu or Fe alloy catalysts for enhancing coke resistance in DRM reactions, our results demonstrate a relatively low conversion tendency for catalysts containing Cu and Fe compared to other components. Although coke resistance remains an important factor to monitor for catalyst stability, the initial reaction conversion was observed to be low, and this finding was further confirmed by the experiments conducted in Section 4.6. A notable observation in the comprehensive heatmap is that the CH_4 conversion values for Ni exhibit a trend of approaching the maximum

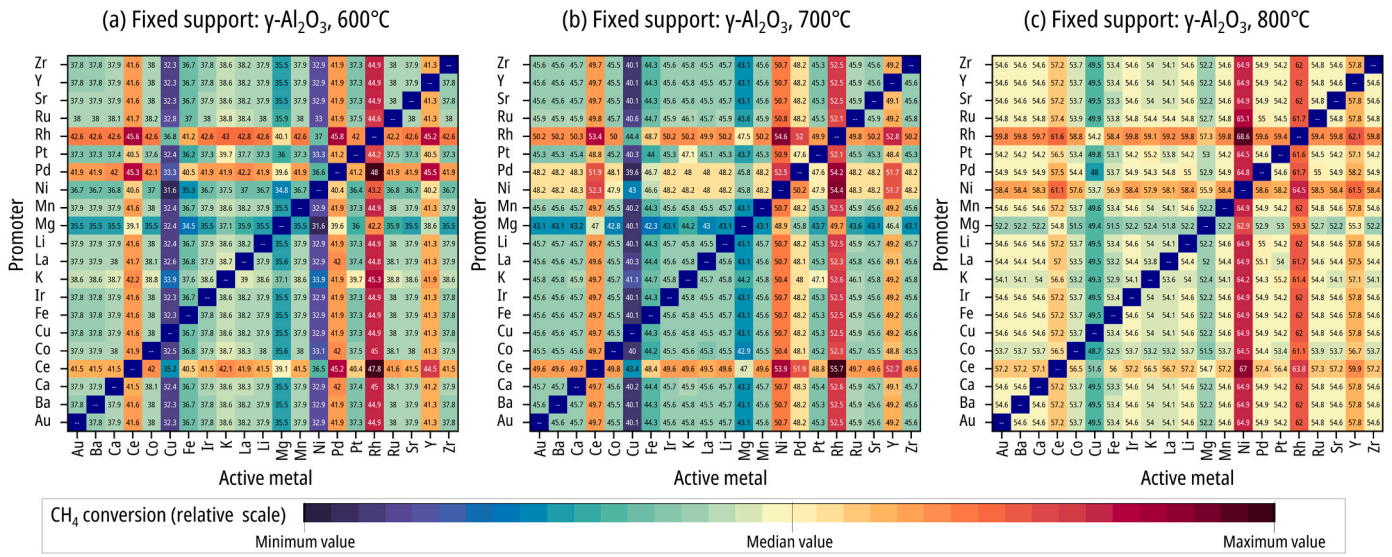

Fig. 8. Predicted CH_4 conversion results based on the generated data.

range at temperatures greater than 700 °C, whereas at temperatures as low as 600 °C, the values tend to be closer to the minimum. This suggests that transition metals, including Ni, demonstrate more effective catalytic activity at temperatures exceeding 600 °C. The results underscore the importance of selecting suitable active metals and promoters for each reaction temperature to maximize the conversion in the DRM reaction, and such selections can be guided by the model.

4.5. Comparison of predicted results and validation experimental results

Fig. 9 shows a graph comparing the model's predicted performance results to the experimental results for the recommended catalyst candidates using the framework proposed in this study. The experimental results align with findings reported in multiple literature sources, demonstrating that the conversion of CH_4 is lower than the conversion of CO_2 because of the occurrence of the reverse water gas shift reaction, which is one of the side reactions in DRM reactions. This alignment verifies the accurate execution of the experiments. Additionally, for the Ni(3)-Ca(2)/Pr_XO_Y-Al_2O_3 catalyst, which was excluded from the training data and not previously reported in the literature, a relatively large difference of approximately 10% existed between the predicted and experimental values. However, it is noteworthy that a difference of 10% remains within the acceptable range of experimental error range. This emphasizes the significance of employing reliable and consistent protocols to obtain high-quality data for the training dataset to achieve precise predictions. An intriguing aspect that emerged unexpectedly in the study is the notable disparities observed in the CH_4 conversion results versus the CO_2 conversion results for the Ce(5)/Y_XO_Y-SiO_2 and Fe(5)-Y(5)/SiO_2 catalysts, indicating the presence of significant errors. Considering the direct reaction between CH_4 and CO_2 to produce the syngas in DRM reactions, the conversion of both reactants should ideally occur in a stoichiometric ratio. Thus, the indirect inference can be drawn from the CO_2 conversion, which reflects the expected stoichiometric ratio of reactant conversion in DRM reactions responsible for syngas production. The notable disparities between the observed CH_4 and CO_2 conversion results for the Ce(5)/Y_XO_Y-SiO_2 and Fe(5)-Y(5)/SiO_2 catalysts indicate their unsuitability for the DRM reaction. This insight highlights the limitations of these catalysts in achieving the desired conversion outcomes and underscores the importance of accurate predictions. Moreover, it demonstrates that the model's predictions are better than a simplistic representation of CH_4 conversion and align more closely with the practical conversion expectations of the reaction. These accurate predictions are achieved by capturing patterns from extensive literature data, highlighting the potential of data-driven models in precisely estimating the desired conversion as anticipated by researchers. We expect that the developed framework can result in

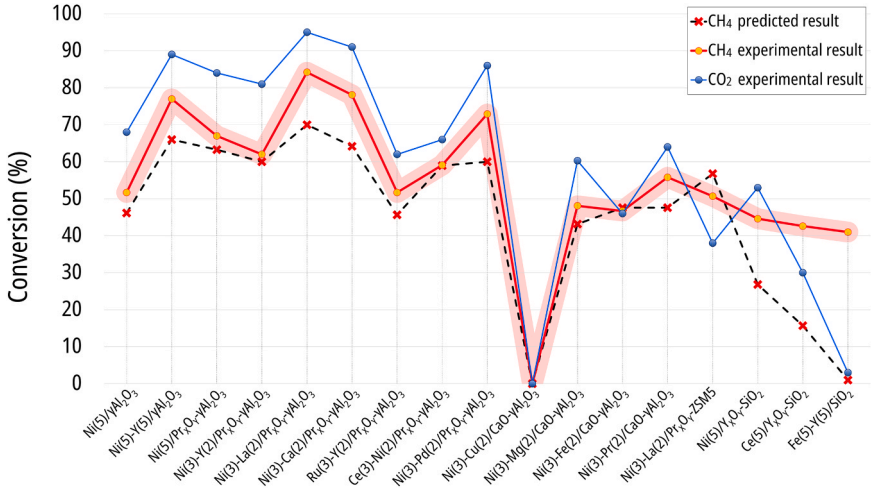

Fig. 9. Comparison of experimental and predicted values for recommended catalyst candidates.

accurate predictions and improved practical conversion results suitable for future catalyst design in many targeted reactions.

5. Conclusions

In this study, we propose the development of an IML model framework to reduce trial and error in the rational design and experimental screening of catalysts. The IML framework addresses the fundamental issue of trustworthiness in the prediction results of black box machine learning models. We specifically apply this framework to the development of DRM catalysts, which are gaining attention as an eco-friendly and alternative energy production option. Furthermore, we conduct verification experiments to validate the effectiveness of the framework.

The dataset required for model development comprised 6067 data points extracted from 132 papers related to DRM catalysts. To understand the causal relationships and contributions between the input and output variables, which are difficult to interpret in black box models, the dataset was preprocessed using IML tools such as SHAP and PDV. The developed model utilized the preprocessed dataset, where appropriate algorithms were selected and hyperparameters were tuned to complete the model development. The generated dataset was then used to create a surrogate model for recommending catalyst candidates. By reducing the influence of catalyst preprocessing and operating conditions and increasing the impact of material design variables on CH_4 conversion, the generated dataset was used to predict the performance of catalyst candidates. The validity of the generated dataset and the ML model was examined using IML tools to perform an interpretability analysis of the model's results. The changes in the results based on the model's variables were refined through global visualization and a model-agnostic approach using IML. The proposed framework not only utilizes IML tools appropriately throughout the steps but also minimizes the influence of catalyst preprocessing conditions, reaction temperature, and other operating conditions, enabling the optimal design of catalyst materials. Additionally, the framework recommends promising DRM catalyst candidates based on the model and provides insights into the impact of variables on the performance of DRM catalysts.

Furthermore, the potential implications of the model's prediction results when expanded to stability and deactivation predictions for DRM catalysts and other reactions, without violating existing domain knowledge, are expected to be promising.

The novelty and key contributions of this research are as follows:

i) Expansion of the exploration space for predicting the performance of DRM catalysts by using a wider range of design variables.
ii) Provision of guidelines for the development of interpretable machine learning models by appropriately using IML tools for the development and interpretation of ML models for catalyst performance prediction.
iii) Recommendation of DRM catalyst candidates using a surrogate model created from a separate dataset, rather than DFT calculation data, and validation of the recommended results through experiments. To the best of our knowledge, no previous study covered the entire process from recommendation to validation experiments for the development of DRM catalysts.
iv) Provision of insights and guidelines by generating datasets that include operating and preprocessing variables under controlled conditions and analyses of the combinations of catalyst design variables, which are difficult to obtain through experimental protocols, to assist researchers.

We anticipate that the academic value of the framework proposed in this study can be further enhanced by associating it to performance metrics required in the industry, such as stability and syngas ratio, through literature data and validation experiments.

CRediT authorship contribution statement

Jiwon Roh[1]: Conceptualization, Data curation, Validation, Writing – original draft, Visualization. **Hyundo Park:** Conceptualization, Methodology, Writing – original draft, Visualization. **Hyukwon Kwon:** Conceptualization, Methodology, Writing – original draft, Visualization. **Chonghyo Joo:** Conceptualization, Data curation, Investigation, Validation, Writing – original draft. **Il Moon:** Methodology, Validation, Writing – review & editing. **Hyungtae Cho:** Methodology, Validation, Writing – review & editing. **Insoo Ro*:** Conceptualization, Writing – review & editing, Supervision, Funding acquisition. **Junghwan Kim*:** Conceptualization, Writing – review & editing, Supervision, Funding acquisition.

Declaration of Competing Interest

The authors declare that they have no known competing financial interests or personal relationships that could have appeared to influence the work reported in this paper.

Data Availability

Data will be made available on request.

Acknowledgment

This work was supported by the Technology Innovation Program funded by the Ministry of Trade, Industry & Energy (MOTIE, South Korea) (Grant No. 00144098, "Development and application of carbon-neutral engineering platform based on carbon emission database and prediction model."). This work was also supported by the Korea Institute of Industrial Technology (KITECH, South Korea) (Grant No. KM-22-0015, "Development and application of AI based microbubble-scrubber system for simultaneous removal of air pollutants."). Additionally, this work was supported by the Korea Environment Industry & Technology Institute (KEITI) through the Center for plasma process for organic material recycling project, funded by the Korea Ministry of Environment (MOE, South Korea) (Grant No. 2022003650002).”

Appendix A. Supporting information

Supplementary data associated with this article can be found in the online version at doi:10.1016/j.apcatb.2023.123454.

References

[1] A. Vojvodic, J.K. Nørskov, New design paradigm for heterogeneous catalysts, Natl. Sci. Rev. 2 (2015) 140–143, https://doi.org/10.1093/nsr/nwv023.
[2] J.K. Nørskov, M. Scheffler, H. Toulhoat, Density functional theory in surface science and heterogeneous catalysis, MRS Bull. 31 (2006) 669–674.
[3] M. Foscato, V.R. Jensen, Automated in silico design of homogeneous catalysts, ACS, Catalysis 10 (2020) 2354–2377.
[4] J. Xu, X.-M. Cao, P. Hu, Perspective on computational reaction prediction using machine learning methods in heterogeneous catalysis, Phys. Chem. Chem. Phys. 23 (2021) 11155–11179.
[5] N.A.K. Aramouni, J.G. Touma, B.A. Tarboush, J. Zeaiter, M.N. Ahmad, Catalyst design for dry reforming of methane: Analysis review, Renew. Sustain. Energy Rev. 82 (2018) 2570–2585.
[6] R. Rapier, Estimating the Carbon Footprint of Hydrogen Production, Retrieved from Forbes: Https://Www. Forbes. Com/Sites/Rrapier/2020/06/06/Estimating-the-Carbon-Footprintof-Hydrogen-Production. (2020).
[7] R. Soltani, M.A. Rosen, I. Dincer, Assessment of CO_2 capture options from various points in steam methane reforming for hydrogen production, Int. J. Hydrog. Energy 39 (2014) 20266–20275, https://doi.org/10.1016/j.ijhydene.2014.09.161.
[8] O. Muraza, A. Galadima, A review on coke management during dry reforming of methane, Int. J. Energy Res. 39 (2015) 1196–1216.
[9] K. Wittich, M. Krämer, N. Bottke, S.A. Schunk, Catalytic dry reforming of methane: insights from model systems, ChemCatChem 12 (2020) 2130–2147.
[10] R. Zhou, N. Mahinpey, A review on catalyst development for conventional thermal dry reforming of methane at low temperature, Can. J. Chem. Eng. (2023).

[11] U. Guharoy, T.R. Reina, J. Liu, Q. Sun, S. Gu, Q. Cai, A theoretical overview on the prevention of coking in dry reforming of methane using non-precious transition metal catalysts, J. CO_2 Util. 53 (2021), 101728, https://doi.org/10.1016/j.jcou.2021.101728.

[12] I.V. Yentekakis, P. Panagiotopoulou, G. Artemakis, A review of recent efforts to promote dry reforming of methane (DRM) to syngas production via bimetallic catalyst formulations, Appl. Catal. B: Environ. 296 (2021), 120210, https://doi.org/10.1016/j.apcatb.2021.120210.

[13] Z. Qin, J. Chen, X. Xie, X. Luo, T. Su, H. Ji, CO 2 reforming of CH 4 to syngas over nickel-based catalysts, Environ. Chem. Lett. 18 (2020) 997–1017.

[14] Y. Yoon, H.M. You, H.J. Kim, M.T. Curnan, K. Kim, J.W. Han, Computational catalyst design for dry reforming of methane: a review, Energy Fuels 36 (2022) 9844–9865, https://doi.org/10.1021/acs.energyfuels.2c01776.

[15] T. Toyao, Z. Maeno, S. Takakusagi, T. Kamachi, I. Takigawa, K.I. Shimizu, Machine learning for catalysis informatics: recent applications and prospects, ACS Catal. 10 (2020) 2260–2297, https://doi.org/10.1021/acscatal.9b04186.

[16] J.A. Esterhuizen, B.R. Goldsmith, S. Linic, Interpretable machine learning for knowledge generation in heterogeneous catalysis, Nat. Catal. 5 (2022) 175–184.

[17] A. Chakkingal, P. Janssens, J. Poissonnier, M. Virginie, A.Y. Khodakov, J. W. Thybaut, Multi-output machine learning models for kinetic data evaluation: a Fischer–Tropsch synthesis case study, Chem. Eng. J. (2022), 137186, https://doi.org/10.1016/j.cej.2022.137186.

[18] A. Nandy, C. Duan, H.J. Kulik, Audacity of huge: overcoming challenges of data scarcity and data quality for machine learning in computational materials discovery, Curr. Opin. Chem. Eng. 36 (2022), 100778, https://doi.org/10.1016/j.coche.2021.100778.

[19] E. Musa, F. Doherty, B.R. Goldsmith, Accelerating the structure search of catalysts with machine learning, Curr. Opin. Chem. Eng. 35 (2022), 100771, https://doi.org/10.1016/j.coche.2021.100771.

[20] C.H. Lee, S. Pahari, N. Sitapure, M.A. Barteau, J.S.-I. Kwon, DFT–kMC analysis for identifying novel bimetallic electrocatalysts for enhanced NRR performance by suppressing HER at ambient conditions via active-site separation, ACS Catal. 12 (2022) 15609–15617.

[21] C.H. Lee, S. Pahari, N. Sitapure, M.A. Barteau, J.S.-I. Kwon, Investigating high-performance non-precious transition metal oxide catalysts for nitrogen reduction reaction: a multifaceted DFT–kMC–LSTM approach, ACS Catal. 13 (2023) 8336–8346.

[22] J. Jiménez-Luna, F. Grisoni, G. Schneider, Drug discovery with explainable artificial intelligence, Nat. Mach. Intell. 2 (2020) 573–584.

[23] M. Langer, D. Oster, T. Speith, H. Hermanns, L. Kästner, E. Schmidt, A. Sesing, K. Baum, What do we want from Explainable Artificial Intelligence (XAI)? – a stakeholder perspective on XAI and a conceptual model guiding interdisciplinary XAI research, Artif. Intell. 296 (2021), 103473, https://doi.org/10.1016/J.ARTINT.2021.103473.

[24] C. Joo, H. Park, J. Lim, H. Cho, J. Kim, Development of physical property prediction models for polypropylene composites with optimizing random forest hyperparameters, Int. J. Intell. Syst. 6 (2022) 3625–3653.

[25] J. Lim, S. Jeong, J. Kim, Deep neural network-based optimal selection and blending ratio of waste seashells as an alternative to high-grade limestone depletion for SOX capture and utilization, Chem. Eng. J. 431 (2022), 133244, https://doi.org/10.1016/J.CEJ.2021.133244.

[26] J. Lee, S. Hong, H. Cho, B. Lyu, M. Kim, J. Kim, I. Moon, Machine learning-based energy optimization for on-site SMR hydrogen production, Energy Convers. Manag. 244 (2021), 114438, https://doi.org/10.1016/J.ENCONMAN.2021.114438.

[27] A. Smith, A. Keane, J.A. Dumesic, G.W. Huber, V.M. Zavala, A machine learning framework for the analysis and prediction of catalytic activity from experimental data, Appl. Catal. B: Environ. 263 (2020), 118257.

[28] H. Kwon, K.C. Oh, Y. Choi, Y.G. Chung, J. Kim, Development and application of machine learning-based prediction model for distillation column, Int. J. Intell. Syst. (2021), https://doi.org/10.1002/int.22368.

[29] A.N. Şener, M.E. Günay, A. Leba, R. Yıldırım, Statistical review of dry reforming of methane literature using decision tree and artificial neural network analysis, Catal. Today 299 (2018) 289–302, https://doi.org/10.1016/j.cattod.2017.05.012.

[30] B.V. Ayodele, C.K. Cheng, Modelling and optimization of syngas production from methane dry reforming over ceria-supported cobalt catalyst using artificial neural networks and Box–Behnken design, J. Ind. Eng. Chem. 32 (2015) 246–258, https://doi.org/10.1016/j.jiec.2015.08.021.

[31] F. ELMAZ, Ö. YÜCEL, A.Y. MUTLU, Predictive modeling of the syngas production from methane dry reforming over cobalt catalyst with statistical and machine learning based approaches, Int. J. Adv. Eng. Pure Sci. 32 (2020) 8–14.

[32] K. Vellayappan, Y. Yue, K.H. Lim, K. Cao, J.Y. Tan, S. Cheng, T. Wang, T.Z. H. Gani, I.A. Karimi, S. Kawi, Impacts of catalyst and process parameters on Ni-catalyzed methane dry reforming via interpretable machine learning, Appl. Catal. B: Environ. 330 (2023), 122593, https://doi.org/10.1016/j.apcatb.2023.122593.

[33] A. Goldstein, A. Kapelner, J. Bleich, E. Pitkin, Peeking inside the black box: visualizing statistical learning with plots of individual conditional expectation, J. Comput. Graph. Stat. 24 (2015) 44–65.

[34] K. Takahashi, J. Ohyama, S. Nishimura, J. Fujima, L. Takahashi, T. Uno, T. Taniike, Catalysts informatics: paradigm shift towards data-driven catalyst design, Chem. Commun. 59 (2023) 2222–2238.

[35] B. Yılmaz, B. Oral, R. Yıldırım, Machine learning analysis of catalytic CO_2 methanation, Int. J. Hydrog. Energy (2023), https://doi.org/10.1016/j.ijhydene.2022.12.197.

[36] A. Lazaridou, L.R. Smith, S. Pattisson, N.F. Dummer, J.J. Smit, P. Johnston, G. J. Hutchings, Recognizing the best catalyst for a reaction, Nat. Rev. Chem. 7 (2023) 287–295, https://doi.org/10.1038/s41570-023-00470-5.

[37] T. Mou, H.S. Pillai, S. Wang, M. Wan, X. Han, N.M. Schweitzer, F. Che, H. Xin, Bridging the complexity gap in computational heterogeneous catalysis with machine learning, Nat. Catal. 6 (2023) 122–136, https://doi.org/10.1038/s41929-023-00911-w.

[38] K. Takahashi, L. Takahashi, T.N. Nguyen, A. Thakur, T. Taniike, Multidimensional Classification of Catalysts in Oxidative Coupling of Methane through Machine Learning and High-Throughput Data, J. Phys. Chem. Lett. 11 (2020) 6819–6826, https://doi.org/10.1021/acs.jpclett.0c01926.

[39] B.V. Ayodele, M.A. Alsaffar, S.I. Mustapa, R. Kanthasamy, S. Wongsakulphasatch, C.K. Cheng, Carbon dioxide reforming of methane over Ni-based catalysts: Modeling the effect of process parameters on greenhouse gasses conversion using supervised machine learning algorithms, Chem. Eng. Process. - Process. Intensif. 166 (2021), 108484, https://doi.org/10.1016/j.cep.2021.108484.

[40] A.N. Şener, M.E. Günay, A. Leba, R. Yıldırım, Statistical review of dry reforming of methane literature using decision tree and artificial neural network analysis, Catal. Today 299 (2018) 289–302, https://doi.org/10.1016/J.CATTOD.2017.05.012.

[41] G. Valderrama, A. Kiennemann, C.U. de Navarro, M.R. Goldwasser, LaNi1-xMnxO3 perovskite-type oxides as catalysts precursors for dry reforming of methane, Appl. Catal. A: Gen. 565 (2018) 26–33, https://doi.org/10.1016/J.APCATA.2018.07.039.

[42] A. Tsoukalou, Q. Imtiaz, S.M. Kim, P.M. Abdala, S. Yoon, C.R. Müller, Dry-reforming of methane over bimetallic Ni–M/La2O3 (M = Co, Fe): The effect of the rate of La2O2CO3 formation and phase stability on the catalytic activity and stability, J. Catal. 343 (2016) 208–214, https://doi.org/10.1016/J.JCAT.2016.03.018.

[43] G. Valderrama, A. Kiennemann, M.R. Goldwasser, La-Sr-Ni-Co-O based perovskite-type solid solutions as catalyst precursors in the CO_2 reforming of methane, J. Power Sources 195 (2010) 1765–1771, https://doi.org/10.1016/J.JPOWSOUR.2009.10.004.

[44] H. Long, Y. Xu, X. Zhang, S. Hu, S. Shang, Y. Yin, X. Dai, Ni-Co/Mg-Al catalyst derived from hydrotalcite-like compound prepared by plasma for dry reforming of methane, J. Energy Chem. 22 (2013) 733–739, https://doi.org/10.1016/S2095-4956(13)60097-2.

[45] H. Ay, D. Üner, Dry reforming of methane over CeO2 supported Ni, Co and Ni–Co catalysts, Appl. Catal. B: Environ. 179 (2015) 128–138, https://doi.org/10.1016/J.APCATB.2015.05.013.

[46] X. Fan, Z. Liu, Y.A. Zhu, G. Tong, J. Zhang, C. Engelbrekt, J. Ulstrup, K. Zhu, X. Zhou, Tuning the composition of metastable CoxNiyMg100−x−y(OH)(OCH3) nanoplates for optimizing robust methane dry reforming catalyst, J. Catal. 330 (2015) 106–119, https://doi.org/10.1016/J.JCAT.2015.06.018.

[47] H. Cheng, S. Feng, W. Tao, X. Lu, W. Yao, G. Li, Z. Zhou, Effects of noble metal-doping on Ni/La2O3–ZrO2 catalysts for dry reforming of coke oven gas, Int. J. Hydrog. Energy 39 (2014) 12604–12612, https://doi.org/10.1016/J.IJHYDENE.2014.06.120.

[48] W.Y. Kim, J.S. Jang, E.C. Ra, K.Y. Kim, E.H. Kim, J.S. Lee, Reduced perovskite LaNiO3 catalysts modified with Co and Mn for low coke formation in dry reforming of methane, Appl. Catal. A: Gen. 575 (2019) 198–203, https://doi.org/10.1016/J.APCATA.2019.02.029.

[49] J.C.S. Wu, H.C. Chou, Bimetallic Rh–Ni/BN catalyst for methane reforming with CO_2, Chem. Eng. J. 148 (2009) 539–545, https://doi.org/10.1016/J.CEJ.2009.01.011.

[50] A. Horváth, G. Stefler, O. Geszti, A. Kienneman, A. Pietraszek, L. Guczi, Methane dry reforming with CO_2 on CeZr-oxide supported Ni, NiRh and NiCo catalysts prepared by sol–gel technique: Relationship between activity and coke formation, Catal. Today 169 (2011) 102–111, https://doi.org/10.1016/J.CATTOD.2010.08.004.

[51] N.H. Elsayed, N.R.M. Roberts, B. Joseph, J.N. Kuhn, Low temperature dry reforming of methane over Pt–Ni–Mg/ceria–zirconia catalysts, Appl. Catal. B: Environ. 179 (2015) 213–219, https://doi.org/10.1016/J.APCATB.2015.05.021.

[52] K. Sheng, D. Luan, H. Jiang, F. Zeng, B. Wei, F. Pang, J. Ge, Ni x Co y Nanocatalyst Supported by ZrO2 Hollow Sphere for Dry Reforming of Methane: Synergetic Catalysis by Ni and Co in Alloy, ACS Appl. Mater. Interfaces 11 (2019) 24078–24087.

[53] X. Song, X. Dong, S. Yin, M. Wang, M. Li, H. Wang, Effects of Fe partial substitution of La2NiO4/LaNiO3 catalyst precursors prepared by wet impregnation method for the dry reforming of methane, Appl. Catal. A: Gen. 526 (2016) 132–138, https://doi.org/10.1016/J.APCATA.2016.07.024.

[54] M. Mousavi, A.N. Pour, Performance and structural features of LaNi 0.5 Co 0.5 O 3 perovskite oxides for the dry reforming of methane: influence of the preparation method, N. J. Chem. 43 (2019) 10763–10773.

[55] X. Yu, F. Zhang, N. Wang, S. Hao, W. Chu, Plasma-treated bimetallic Ni–Pt catalysts derived from hydrotalcites for the carbon dioxide reforming of methane, Catal. Lett. 144 (2014) 293–300, https://doi.org/10.1007/s10562-013-1130-3.

[56] M.A. Vasiliades, C.M. Damaskinos, K.K. Kyprianou, M. Kollia, A.M. Efstathiou, The effect of Pt on the carbon pathways in the dry reforming of methane over Ni-Pt/Ce0.8Pr0.2O2-δ catalyst, Catal. Today 355 (2020) 788–803, https://doi.org/10.1016/J.CATTOD.2019.04.022.

[57] M.R. Goldwasser, M.E. Rivas, E. Pietri, M.J. Pérez-Zurita, M.L. Cubeiro, A. Grivobal-Constant, G. Leclercq, Perovskites as catalysts precursors: synthesis and characterization, J. Mol. Catal. A: Chem. 228 (2005) 325–331, https://doi.org/10.1016/J.MOLCATA.2004.09.030.

[58] F. Touahra, R. Chebout, D. Lerari, D. Halliche, K. Bachari, Role of the nanoparticles of Cu-Co alloy derived from perovskite in dry reforming of methane, Energy 171 (2019) 465–474, https://doi.org/10.1016/J.ENERGY.2019.01.085.

[59] C. Batiot-Dupeyrat, G.A.S. Gallego, F. Mondragon, J. Barrault, J.M. Tatibouët, CO_2 reforming of methane over LaNiO3 as precursor material, Catal. Today 107–108 (2005) 474–480, https://doi.org/10.1016/J.CATTOD.2005.07.014.

[60] V.R. Choudhary, K.C. Mondal, A.S. Mamman, U.A. Joshi, Carbon-free dry reforming of methane to syngas over NdCoO3 perovskite-type mixed metal oxide catalyst, Catal. Lett. 100 (2005) 271–276.

[61] S.K. Chawla, M. George, F. Patel, S. Patel, Production of synthesis gas by carbon dioxide reforming of methane over nickel based and perovskite catalysts, Procedia Eng. 51 (2013) 461–466, https://doi.org/10.1016/J.PROENG.2013.01.065.

[62] T.C. Feng, W.T. Zheng, K.Q. Sun, B.Q. Xu, CO_2 reforming of methane over coke-resistant Ni–Co/Si3N4 catalyst prepared via reactions between silicon nitride and metal halides, Catal. Commun. 73 (2016) 54–57, https://doi.org/10.1016/J.CATCOM.2015.10.009.

[63] J. Estephane, S. Aouad, S. Hany, B. El Khoury, C. Gennequin, H. El Zakhem, J. El Nakat, A. Aboukaïs, E. Abi Aad, CO_2 reforming of methane over Ni–Co/ZSM5 catalysts. Aging and carbon deposition study, Int. J. Hydrog. Energy 40 (2015) 9201–9208, https://doi.org/10.1016/J.IJHYDENE.2015.05.147.

[64] S. Mine, M. Takao, T. Yamaguchi, T. Toyao, Z. Maeno, S.M.A. Hakim Siddiki, S. Takakusagi, K. ichi Shimizu, I. Takigawa, Analysis of Updated Literature Data up to 2019 on the Oxidative Coupling of Methane Using an Extrapolative Machine-Learning Method to Identify Novel Catalysts, ChemCatChem 13 (2021) 3636–3655, https://doi.org/10.1002/cctc.202100495.

[65] A.S.A. Al-Fatesh, A.H. Fakeeha, Effects of calcination and activation temperature on dry reforming catalysts, J. Saudi Chem. Soc. 16 (2012) 55–61, https://doi.org/10.1016/J.JSCS.2010.10.020.

[66] Y.X. Pan, C.J. Liu, P. Shi, Preparation and characterization of coke resistant Ni/SiO2 catalyst for carbon dioxide reforming of methane, J. Power Sources 176 (2008) 46–53, https://doi.org/10.1016/J.JPOWSOUR.2007.10.039.

[67] R. Shang, X. Guo, S. Mu, Y. Wang, G. Jin, H. Kosslick, A. Schulz, X.Y. Guo, Carbon dioxide reforming of methane to synthesis gas over Ni/Si3N4 catalysts, Int. J. Hydrog. Energy 36 (2011) 4900–4907, https://doi.org/10.1016/J.IJHYDENE.2011.01.034.

[68] A. Ballarini, F. Basile, P. Benito, I. Bersani, G. Fornasari, S. De Miguel, S.C. P. Maina, J. Vilella, A. Vaccari, O.A. Scelza, Platinum supported on alkaline and alkaline earth metal-doped alumina as catalysts for dry reforming and partial oxidation of methane, Appl. Catal. A: General. 433–434 (2012) 1–11, https://doi.org/10.1016/J.APCATA.2012.04.037.

[69] D. Halliche, O. Cherifi, A. Auroux, Microcalorimetric studies and methane reforming by CO_2 on Ni-based zeolite catalysts, Thermochim. Acta 434 (2005) 125–131, https://doi.org/10.1016/J.TCA.2005.01.005.

[70] J. Newnham, K. Mantri, M.H. Amin, J. Tardio, S.K. Bhargava, Highly stable and active Ni-mesoporous alumina catalysts for dry reforming of methane, Int. J. Hydrog. Energy 37 (2012) 1454–1464, https://doi.org/10.1016/J.IJHYDENE.2011.10.036.

[71] A. Moniri, S.M. Alavi, M. Rezaei, Syngas production by combined carbon dioxide reforming and partial oxidation of methane over Ni/α-Al2O3 catalysts, J. Nat. Gas. Chem. 19 (2010) 638–641, https://doi.org/10.1016/S1003-9953(09)60127-4.

[72] I. Tankov, K. Arishtirova, J.M.C. Bueno, S. Damyanova, Surface and structural features of Pt/PrO2–Al2O3 catalysts for dry methane reforming, Appl. Catal. A: Gen. 474 (2014) 135–148, https://doi.org/10.1016/J.APCATA.2013.08.030.

[73] R. Zanganeh, M. Rezaei, A. Zamaniyan, H.R. Bozorgzadeh, Preparation of Ni0.1Mg0. 9O nanocrystalline powder and its catalytic performance in methane reforming with carbon dioxide, J. Ind. Eng. Chem. 19 (2013) 234–239.

[74] N. Wang, X. Yu, K. Shen, W. Chu, W. Qian, Synthesis, characterization and catalytic performance of MgO-coated Ni/SBA-15 catalysts for methane dry reforming to syngas and hydrogen, Int. J. Hydrog. Energy 38 (2013) 9718–9731, https://doi.org/10.1016/J.IJHYDENE.2013.05.097.

[75] H. Wu, G. Pantaleo, V. La Parola, A.M. Venezia, X. Collard, C. Aprile, L.F. Liotta, Bi- and trimetallic Ni catalysts over Al2O3 and Al2O3-MOx (M = Ce or Mg) oxides for methane dry reforming: Au and Pt additive effects, Appl. Catal. B: Environ. 156–157 (2014) 350–361, https://doi.org/10.1016/J.APCATB.2014.03.018.

[76] J.D.A. Bellido, J.E. De Souza, J.C. M'Peko, E.M. Assaf, Effect of adding CaO to ZrO2 support on nickel catalyst activity in dry reforming of methane, Appl. Catal. A: Gen. 358 (2009) 215–223, https://doi.org/10.1016/J.APCATA.2009.02.014.

[77] B. Nematollahi, M. Rezaei, M. Khajenoori, Combined dry reforming and partial oxidation of methane to synthesis gas on noble metal catalysts, Int. J. Hydrog. Energy 36 (2011) 2969–2978, https://doi.org/10.1016/J.IJHYDENE.2010.12.007.

[78] Ş. Özkara-Aydinoğlu, A.E. Aksoylu, Carbon dioxide reforming of methane over Co-X/ZrO2 catalysts (X = La, Ce, Mn, Mg, K), Catal. Commun. 11 (2010) 1165–1170, https://doi.org/10.1016/J.CATCOM.2010.07.001.

[79] M. Tang, L. Xu, M. Fan, Effect of Ce on 5 wt% Ni/ZSM-5 catalysts in the CO_2 reforming of CH4 reaction, Int. J. Hydrog. Energy 39 (2014) 15482–15496, https://doi.org/10.1016/J.IJHYDENE.2014.07.172.

[80] A.I. Tsyganok, M. Inaba, T. Tsunoda, K. Uchida, K. Suzuki, K. Takehira, T. Hayakawa, Rational design of Mg–Al mixed oxide-supported bimetallic catalysts for dry reforming of methane, Appl. Catal. A: Gen. 292 (2005) 328–343, https://doi.org/10.1016/J.APCATA.2005.06.007.

[81] J.S. Chang, D.Y. Hong, X. Li, S.E. Park, Thermogravimetric analyses and catalytic behaviors of zirconia-supported nickel catalysts for carbon dioxide reforming of methane, Catal. Today 115 (2006) 186–190, https://doi.org/10.1016/J.CATTOD.2006.02.052.

[82] A.H. Fakeeha, M.A. Naeem, W.U. Khan, A.S. Al-Fatesh, Syngas production via CO_2 reforming of methane using Co-Sr-Al catalyst, J. Ind. Eng. Chem. 20 (2014) 549–557, https://doi.org/10.1016/J.JIEC.2013.05.013.

[83] G.R. Moradi, F. Khosravian, M. Rahmanzadeh, Effects of Partial Substitution of Ni by Cu in LaNiO3 Perovskite Catalyst for Dry Methane Reforming, Chin. J. Catal. 33 (2012) 797–801, https://doi.org/10.1016/S1872-2067(11)60378-1.

[84] G.S. Gallego, F. Mondragón, J. Barrault, J.M. Tatibouët, C. Batiot-Dupeyrat, CO_2 reforming of CH4 over La–Ni based perovskite precursors, Appl. Catal. A: Gen. 311 (2006) 164–171, https://doi.org/10.1016/J.APCATA.2006.06.024.

[85] I. Luisetto, S. Tuti, E. Di Bartolomeo, Co and Ni supported on CeO2 as selective bimetallic catalyst for dry reforming of methane, Int. J. Hydrog. Energy 37 (2012) 15992–15999, https://doi.org/10.1016/J.IJHYDENE.2012.08.006.

[86] A.R. González, Y.J.O. Asencios, E.M. Assaf, J.M. Assaf, Dry reforming of methane on Ni–Mg–Al nano-spheroid oxide catalysts prepared by the sol–gel method from hydrotalcite-like precursors, Appl. Surf. Sci. 280 (2013) 876–887, https://doi.org/10.1016/J.APSUSC.2013.05.082.

[87] A. Kambolis, H. Matralis, A. Trovarelli, C. Papadopoulou, Ni/CeO2-ZrO2 catalysts for the dry reforming of methane, Appl. Catal. A: Gen. 377 (2010) 16–26, https://doi.org/10.1016/J.APCATA.2010.01.013.

[88] R. Zanganeh, M. Rezaei, A. Zamaniyan, Dry reforming of methane to synthesis gas on NiO–MgO nanocrystalline solid solution catalysts, Int. J. Hydrog. Energy 38 (2013) 3012–3018, https://doi.org/10.1016/J.IJHYDENE.2012.12.089.

[89] A. Nandini, K.K. Pant, S.C. Dhingra, K-, CeO2-, and Mn-promoted Ni/Al2O3 catalysts for stable CO_2 reforming of methane, Appl. Catal. A: Gen. 290 (2005) 166–174, https://doi.org/10.1016/J.APCATA.2005.05.016.

[90] M. Zhang, S. Ji, L. Hu, F. Yin, C. Li, H. Liu, Structural Characterization of Highly Stable Ni/SBA-15 Catalyst and Its Catalytic Performance for Methane Reforming with CO_2, Chin. J. Catal. 27 (2006) 777–781, https://doi.org/10.1016/S1872-2067(06)60043-0.

[91] M. García-Diéguez, I.S. Pieta, M.C. Herrera, M.A. Larrubia, L.J. Alemany, Improved Pt-Ni nanocatalysts for dry reforming of methane, Appl. Catal. A: Gen. 377 (2010) 191–199, https://doi.org/10.1016/J.APCATA.2010.01.038.

[92] S. Damyanova, B. Pawelec, K. Arishtirova, M.V.M. Huerta, J.L.G. Fierro, The effect of CeO2 on the surface and catalytic properties of Pt/CeO2–ZrO2 catalysts for methane dry reforming, Appl. Catal. B: Environ. 89 (2009) 149–159, https://doi.org/10.1016/J.APCATB.2008.11.035.

[93] Ş. Özkara-Aydinoğlu, E. Özensoy, A.E. Aksoylu, The effect of impregnation strategy on methane dry reforming activity of Ce promoted Pt/ZrO2, Int. J. Hydrog. Energy 34 (2009) 9711–9722, https://doi.org/10.1016/J.IJHYDENE.2009.09.005.

[94] M. Rezaei, S.M. Alavi, S. Sahebdelfar, Z.F. Yan, A highly stable catalyst in methane reforming with carbon dioxide, Scr. Mater. 61 (2009) 173–176, https://doi.org/10.1016/J.SCRIPTAMAT.2009.03.033.

[95] Y.H. Taufiq-Yap, Sudarno, U. Rashid, Z. Zainal, CeO2–SiO2 supported nickel catalysts for dry reforming of methane toward syngas production, Appl. Catal. A: Gen. 468 (2013) 359–369, https://doi.org/10.1016/J.APCATA.2013.09.020.

[96] B. Nematollahi, M. Rezaei, M. Asghari, A. Fazeli, E.N. Lay, F. Nematollahi, A comparative study between modeling and experimental results over rhodium supported catalyst in dry reforming reaction, Fuel 134 (2014) 565–572, https://doi.org/10.1016/J.FUEL.2014.05.093.

[97] M.A. Naeem, A.S. Al-Fatesh, A.E. Abasaeed, A.H. Fakeeha, Activities of Ni-based nano catalysts for CO_2–CH4 reforming prepared by polyol process, Fuel Process. Technol. 122 (2014) 141–152, https://doi.org/10.1016/J.FUPROC.2014.01.035.

[98] G.K. Reddy, S. Loridant, A. Takahashi, P. Delichère, B.M. Reddy, Reforming of methane with carbon dioxide over Pt/ZrO2/SiO2 catalysts—Effect of zirconia to silica ratio, Appl. Catal. A: Gen. 389 (2010) 92–100, https://doi.org/10.1016/J.APCATA.2010.09.007.

[99] F. Meshkani, M. Rezaei, Nanocrystalline MgO supported nickel-based bimetallic catalysts for carbon dioxide reforming of methane, Int. J. Hydrog. Energy 35 (2010) 10295–10301, https://doi.org/10.1016/J.IJHYDENE.2010.07.138.

[100] F. Meshkani, M. Rezaei, M. Andache, Investigation of the catalytic performance of Ni/MgO catalysts in partial oxidation, dry reforming and combined reforming of methane, J. Ind. Eng. Chem. 20 (2014) 1251–1260, https://doi.org/10.1016/J.JIEC.2013.06.052.

[101] S. Zhang, J. Wang, X. Wang, Effect of calcination temperature on structure and performance of Ni/TiO2-SiO2 catalyst for CO_2 reforming of methane, J. Nat. Gas Chem. 17 (2008) 179–183, https://doi.org/10.1016/S1003-9953(08)60048-1.

[102] R. Zanganeh, M. Rezaei, A. Zamaniyan, Preparation of nanocrystalline NiO–MgO solid solution powders as catalyst for methane reforming with carbon dioxide: effect of preparation conditions, Adv. Powder Technol. 25 (2014) 1111–1117, https://doi.org/10.1016/J.APT.2014.02.015.

[103] B.M. Nagaraja, D.A. Bulushev, S. Beloshapkin, J.R.H. Ross, The effect of potassium on the activity and stability of Ni–MgO–ZrO2 catalysts for the dry reforming of methane to give synthesis gas, Catal. Today 178 (2011) 132–136, https://doi.org/10.1016/J.CATTOD.2011.08.040.

[104] K. Takanabe, K. Nagaoka, K. Nariai, K.I. Aika, Influence of reduction temperature on the catalytic behavior of Co/TiO2 catalysts for CH4/CO_2 reforming and its relation with titania bulk crystal structure, J. Catal. 230 (2005) 75–85, https://doi.org/10.1016/J.JCAT.2004.11.005.

[105] A.D. Ballarini, S.R. De Miguel, E.L. Jablonski, O.A. Scelza, A.A. Castro, Reforming of CH4 with CO_2 on Pt-supported catalysts: Effect of the support on the catalytic

behaviour, Catal. Today 107–108 (2005) 481–486, https://doi.org/10.1016/J.CATTOD.2005.07.058.
[106] E.N. Alvar, M. Rezaei, Mesoporous nanocrystalline MgAl2O4 spinel and its applications as support for Ni catalyst in dry reforming, Scr. Mater. 61 (2009) 212–215, https://doi.org/10.1016/J.SCRIPTAMAT.2009.03.047.
[107] F. Mirzaei, M. Rezaei, F. Meshkani, Z. Fattah, Carbon dioxide reforming of methane for syngas production over Co–MgO mixed oxide nanocatalysts, J. Ind. Eng. Chem. 21 (2015) 662–667, https://doi.org/10.1016/J.JIEC.2014.03.034.
[108] M. Ocsachoque, F. Pompeo, G. Gonzalez, Rh–Ni/CeO2–Al2O3 catalysts for methane dry reforming, Catal. Today 172 (2011) 226–231, https://doi.org/10.1016/J.CATTOD.2011.02.057.
[109] V.M. Gonzalez-delaCruz, R. Pereniguez, F. Ternero, J.P. Holgado, A. Caballero, In situ XAS study of synergic effects on Ni–Co/ZrO2 methane reforming catalysts, J. Phys. Chem. C. 116 (2012) 2919–2926.
[110] A. Serrano-Lotina, L. Daza, Influence of the operating parameters over dry reforming of methane to syngas, Int. J. Hydrog. Energy 39 (2014) 4089–4094, https://doi.org/10.1016/J.IJHYDENE.2013.05.135.
[111] J.F. Li, C. Xia, C.T. Au, B.S. Liu, Y2O3-promoted NiO/SBA-15 catalysts highly active for CO_2/CH4 reforming, Int. J. Hydrog. Energy 39 (2014) 10927–10940, https://doi.org/10.1016/J.IJHYDENE.2014.05.021.
[112] A. Ranjbar, M. Rezaei, Dry reforming reaction over nickel catalysts supported on nanocrystalline calcium aluminates with different CaO/Al2O3 ratios, J. Nat. Gas Chem. 21 (2012) 178–183, https://doi.org/10.1016/S1003-9953(11)60351-4.
[113] L. Xu, H. Song, L. Chou, Mesoporous nanocrystalline ceria–zirconia solid solutions supported nickel based catalysts for CO_2 reforming of CH4, Int. J. Hydrog. Energy 37 (2012) 18001–18020, https://doi.org/10.1016/J.IJHYDENE.2012.09.128.
[114] S. Yasyerli, S. Filizgok, H. Arbag, N. Yasyerli, G. Dogu, Ru incorporated Ni–MCM-41 mesoporous catalysts for dry reforming of methane: effects of Mg addition, feed composition and temperature, Int. J. Hydrog. Energy 36 (2011) 4863–4874, https://doi.org/10.1016/J.IJHYDENE.2011.01.120.
[115] S. Sengupta, K. Ray, G. Deo, Effects of modifying Ni/Al2O3 catalyst with cobalt on the reforming of CH4 with CO_2 and cracking of CH4 reactions, Int. J. Hydrog. Energy 39 (2014) 11462–11472, https://doi.org/10.1016/J.IJHYDENE.2014.05.058.
[116] T.D. Gould, M.M. Montemore, A.M. Lubers, L.D. Ellis, A.W. Weimer, J.L. Falconer, J.W. Medlin, Enhanced dry reforming of methane on Ni and Ni-Pt catalysts synthesized by atomic layer deposition, Appl. Catal. A: Gen. 492 (2015) 107–116, https://doi.org/10.1016/J.APCATA.2014.11.037.
[117] R. Wang, X. Liu, Y. Chen, W. Li, H. Xu, Effect of metal–support interaction on coking resistance of Rh-based catalysts in CH4/CO_2 reforming, Chin. J. Catal. 28 (2007) 865–869, https://doi.org/10.1016/S1872-2067(07)60072-2.
[118] S. Pavlova, L. Kapokova, R. Bunina, G. Alikina, N. Sazonova, T. Krieger, A. Ishchenko, V. Rogov, R. Gulyaev, V. Sadykov, Syngas production by CO 2 reforming of methane using LnFeNi (Ru) O 3 perovskites as precursors of robust catalysts, Catal. Sci. Technol. 2 (2012) 2099–2108.
[119] Z. Alipour, M. Rezaei, F. Meshkani, Effect of alkaline earth promoters (MgO, CaO, and BaO) on the activity and coke formation of Ni catalysts supported on nanocrystalline Al2O3 in dry reforming of methane, J. Ind. Eng. Chem. 20 (2014) 2858–2863, https://doi.org/10.1016/J.JIEC.2013.11.018.
[120] L. Xu, H. Zhao, H. Song, L. Chou, Ordered mesoporous alumina supported nickel based catalysts for carbon dioxide reforming of methane, Int. J. Hydrog. Energy 37 (2012) 7497–7511, https://doi.org/10.1016/J.IJHYDENE.2012.01.105.
[121] M.E. Rivas, J.L.G. Fierro, M.R. Goldwasser, E. Pietri, M.J. Pérez-Zurita, A. Griboval-Constant, G. Leclercq, Structural features and performance of LaNi1−xRhxO3 system for the dry reforming of methane, Appl. Catal. A: Gen. 344 (2008) 10–19, https://doi.org/10.1016/J.APCATA.2008.03.023.
[122] J. Juan-Juan, M.C. Román-Martínez, M.J. Illán-Gómez, Effect of potassium content in the activity of K-promoted Ni/Al2O3 catalysts for the dry reforming of methane, Appl. Catal. A: Gen. 301 (2006) 9–15, https://doi.org/10.1016/J.APCATA.2005.11.006.
[123] S. Damyanova, B. Pawelec, K. Arishtirova, J.L.G. Fierro, Biogas reforming over bimetallic PdNi catalysts supported on phosphorus-modified alumina, Int. J. Hydrog. Energy 36 (2011) 10635–10647, https://doi.org/10.1016/J.IJHYDENE.2011.05.098.
[124] F. Pompeo, D. Gazzoli, N.N. Nichio, Stability improvements of Ni/α-Al2O3 catalysts to obtain hydrogen from methane reforming, Int. J. Hydrog. Energy 34 (2009) 2260–2268, https://doi.org/10.1016/J.IJHYDENE.2008.12.057.
[125] W.D. Zhang, B.S. Liu, C. Zhu, Y.L. Tian, Preparation of La2NiO4/ZSM-5 catalyst and catalytic performance in CO_2/CH4 reforming to syngas, Appl. Catal. A: Gen. 292 (2005) 138–143, https://doi.org/10.1016/J.APCATA.2005.05.018.
[126] H. Jiang, X. Yu, R. Nie, X. Lu, D. Zhou, Q. Xia, Selective hydrogenation of aromatic carboxylic acids over basic N-doped mesoporous carbon supported palladium catalysts, Appl. Catal. A: Gen. 520 (2016) 73–81, https://doi.org/10.1016/J.APCATA.2016.04.009.
[127] X. Lv, J.F. Chen, Y. Tan, Y. Zhang, A highly dispersed nickel supported catalyst for dry reforming of methane, Catal. Commun. 20 (2012) 6–11, https://doi.org/10.1016/J.CATCOM.2012.01.002.
[128] K. Takanabe, K. Nagaoka, K. Nariai, K.I. Aika, Titania-supported cobalt and nickel bimetallic catalysts for carbon dioxide reforming of methane, J. Catal. 232 (2005) 268–275, https://doi.org/10.1016/J.JCAT.2005.03.011.
[129] D.G. Araiza, D.G. Arcos, A. Gómez-Cortés, G. Díaz, Dry reforming of methane over Pt-Ni/CeO2 catalysts: Effect of the metal composition on the stability, Catal. Today 360 (2021) 46–54, https://doi.org/10.1016/J.CATTOD.2019.06.018.
[130] B. Pawelec, S. Damyanova, K. Arishtirova, J.L.G. Fierro, L. Petrov, Structural and surface features of PtNi catalysts for reforming of methane with CO_2, Appl. Catal. A: Gen. 323 (2007) 188–201, https://doi.org/10.1016/J.APCATA.2007.02.017.
[131] A.S. Al-Fatesh, M.A. Naeem, A.H. Fakeeha, A.E. Abasaeed, Role of La2O3 as promoter and support in Ni/γ-Al2O3 catalysts for dry reforming of methane, Chin. J. Chem. Eng. 22 (2014) 28–37, https://doi.org/10.1016/S1004-9541(14)60029-X.
[132] J. Xu, W. Zhou, Z. Li, J. Wang, J. Ma, Biogas reforming for hydrogen production over a Ni–Co bimetallic catalyst: Effect of operating conditions, Int. J. Hydrog. Energy 35 (2010) 13013–13020, https://doi.org/10.1016/J.IJHYDENE.2010.04.075.
[133] M. Abdollahifar, M. Haghighi, A.A. Babaluo, Syngas production via dry reforming of methane over Ni/Al2O3–MgO nanocatalyst synthesized using ultrasound energy, J. Ind. Eng. Chem. 20 (2014) 1845–1851, https://doi.org/10.1016/J.JIEC.2013.08.041.
[134] V. García, J.J. Fernández, W. Ruíz, F. Mondragón, A. Moreno, Effect of MgO addition on the basicity of Ni/ZrO2 and on its catalytic activity in carbon dioxide reforming of methane, Catal. Commun. 11 (2009) 240–246, https://doi.org/10.1016/J.CATCOM.2009.10.003.
[135] D. San-José-Alonso, J. Juan-Juan, M.J. Illán-Gómez, M.C. Román-Martínez, Ni, Co and bimetallic Ni–Co catalysts for the dry reforming of methane, Appl. Catal. A: Gen. 371 (2009) 54–59, https://doi.org/10.1016/J.APCATA.2009.09.026.
[136] D. San José-Alonso, M.J. Illán-Gómez, M.C. Román-Martínez, K and Sr promoted Co alumina supported catalysts for the CO_2 reforming of methane, Catal. Today 176 (2011) 187–190, https://doi.org/10.1016/J.CATTOD.2010.11.093.
[137] N. Hadian, M. Rezaei, Z. Mosayebi, F. Meshkani, CO_2 reforming of methane over nickel catalysts supported on nanocrystalline MgAl2O4 with high surface area, J. Nat. Gas. Chem. 21 (2012) 200–206, https://doi.org/10.1016/S1003-9953(11)60355-1.
[138] A. Luengnaruemitchai, A. Kaengsilalai, Activity of different zeolite-supported Ni catalysts for methane reforming with carbon dioxide, Chem. Eng. J. 144 (2008) 96–102, https://doi.org/10.1016/J.CEJ.2008.05.023.
[139] S. Therdthianwong, C. Siangchin, A. Therdthianwong, Improvement of coke resistance of Ni/Al2O3 catalyst in CH4/CO_2 reforming by ZrO2 addition, Fuel Process. Technol. 89 (2008) 160–168, https://doi.org/10.1016/J.FUPROC.2007.09.003.
[140] M. Yang, H. Papp, CO_2 reforming of methane to syngas over highly active and stable Pt/MgO catalysts, Catal. Today 115 (2006) 199–204, https://doi.org/10.1016/J.CATTOD.2006.02.047.
[141] W.K. Jóźwiak, M. Nowosielska, J. Rynkowski, Reforming of methane with carbon dioxide over supported bimetallic catalysts containing Ni and noble metal: I. Characterization and activity of SiO2 supported Ni–Rh catalysts, Appl. Catal. A: Gen. 280 (2005) 233–244, https://doi.org/10.1016/J.APCATA.2004.11.003.
[142] F. Meshkani, M. Rezaei, Ni catalysts supported on nanocrystalline magnesium oxide for syngas production by CO_2 reforming of CH4, J. Nat. Gas. Chem. 20 (2011) 198–203, https://doi.org/10.1016/S1003-9953(10)60169-7.
[143] R. Yang, C. Xing, C. Lv, L. Shi, N. Tsubaki, Promotional effect of La2O3 and CeO2 on Ni/γ-Al2O3 catalysts for CO_2 reforming of CH4, Appl. Catal. A: Gen. 385 (2010) 92–100, https://doi.org/10.1016/J.APCATA.2010.06.050.
[144] Y. Vafaeian, M. Haghighi, S. Aghamohammadi, Ultrasound assisted dispersion of different amount of Ni over ZSM-5 used as nanostructured catalyst for hydrogen production via CO_2 reforming of methane, Energy Convers. Manag. 76 (2013) 1093–1103, https://doi.org/10.1016/J.ENCONMAN.2013.08.010.
[145] N. Habibi, M. Rezaei, N. Majidian, M. Andache, CH4 reforming with CO_2 for syngas production over La2O3 promoted Ni catalysts supported on mesoporous nanostructured γ-Al2O3, J. Energy Chem. 23 (2014) 435–442, https://doi.org/10.1016/S2095-4956(14)60169-8.
[146] I. Sarusi, K. Fodor, K. Baán, A. Oszkó, G. Pótári, A. Erdőhelyi, CO_2 reforming of CH4 on doped Rh/Al2O3 catalysts, Catal. Today 171 (2011) 132–139, https://doi.org/10.1016/J.CATTOD.2011.03.075.
[147] M.M. Barroso-Quiroga, A.E. Castro-Luna, Catalytic activity and effect of modifiers on Ni-based catalysts for the dry reforming of methane, Int. J. Hydrog. Energy 35 (2010) 6052–6056, https://doi.org/10.1016/J.IJHYDENE.2009.12.073.
[148] S. Zhang, J. Wang, H. Liu, X. Wang, One-pot synthesis of Ni-nanoparticle-embedded mesoporous titania/silica catalyst and its application for CO_2-reforming of methane, Catal. Commun. 9 (2008) 995–1000, https://doi.org/10.1016/J.CATCOM.2007.09.033.
[149] A.H. Fakeeha, W.U. Khan, A.S. Al-Fatesh, A.E. Abasaeed, Stabilities of zeolite-supported Ni catalysts for dry reforming of methane, Chin. J. Catal. 34 (2013) 764–768, https://doi.org/10.1016/S1872-2067(12)60554-3.
[150] Z. Hou, P. Chen, H. Fang, X. Zheng, T. Yashima, Production of synthesis gas via methane reforming with CO_2 on noble metals and small amount of noble-(Rh-) promoted Ni catalysts, Int. J. Hydrog. Energy 31 (2006) 555–561, https://doi.org/10.1016/J.IJHYDENE.2005.06.010.
[151] R. Bouarab, O. Cherifi, A. Auroux, Effect of the basicity created by La2O3 addition on the catalytic properties of Co(O)/SiO2 in CH4 + CO_2 reaction, Thermochim. Acta 434 (2005) 69–73, https://doi.org/10.1016/J.TCA.2005.01.019.
[152] M. Rezaei, S.M. Alavi, S. Sahebdelfar, Z.F. Yan, Syngas Production by Methane Reforming with Carbon Dioxide on Noble Metal Catalysts, J. Nat. Gas. Chem. 15 (2006) 327–334, https://doi.org/10.1016/S1003-9953(07)60014-0.
[153] A. Al-Fatesh, Suppression of carbon formation in CH4–CO_2 reforming by addition of Sr into bimetallic Ni–Co/γ-Al2O3 catalyst, J. King Saud. Univ. - Eng. Sci. 27 (2015) 101–107, https://doi.org/10.1016/J.JKSUES.2013.09.006.
[154] A.S.A. Al-Fatesh, A.H. Fakeeha, A.E. Abasaeed, Effects of Selected Promoters on Ni/Y-Al2O3 Catalyst Performance in Methane Dry Reforming, Chin. J. Catal. 32 (2011) 1604–1609, https://doi.org/10.1016/S1872-2067(10)60267-7.
[155] J.H. Lee, Y.W. You, H.C. Ahn, J.S. Hong, S.B. Kim, T.S. Chang, J.K. Suh, The deactivation study of Co–Ru–Zr catalyst depending on supports in the dry

reforming of carbon dioxide, J. Ind. Eng. Chem. 20 (2014) 284–289, https://doi.org/10.1016/J.JIEC.2013.03.036.
[156] M. García-Diéguez, I.S. Pieta, M.C. Herrera, M.A. Larrubia, L.J. Alemany, Nanostructured Pt- and Ni-based catalysts for CO_2-reforming of methane, J. Catal. 270 (2010) 136–145, https://doi.org/10.1016/J.JCAT.2009.12.010.
[157] M. Rezaei, S.M. Alavi, S. Sahebdelfar, P. Bai, X. Liu, Z.F. Yan, CO_2 reforming of CH4 over nanocrystalline zirconia-supported nickel catalysts, Appl. Catal. B: Environ. 77 (2008) 346–354, https://doi.org/10.1016/J.APCATB.2007.08.004.
[158] Ş. Özkara-Aydnolu, A.E. Aksoylu, CO_2 reforming of methane over Pt–Ni/Al2O3 catalysts: effects of catalyst composition, and water and oxygen addition to the feed, Int. J. Hydrog. Energy 36 (2011) 2950–2959, https://doi.org/10.1016/J.IJHYDENE.2010.11.080.
[159] L. Yao, J. Zhu, X. Peng, D. Tong, C. Hu, Comparative study on the promotion effect of Mn and Zr on the stability of Ni/SiO2 catalyst for CO_2 reforming of methane, Int. J. Hydrog. Energy 38 (2013) 7268–7279, https://doi.org/10.1016/J.IJHYDENE.2013.02.126.
[160] M. García-Diéguez, E. Finocchio, M.Á. Larrubia, L.J. Alemany, G. Busca, Characterization of alumina-supported Pt, Ni and PtNi alloy catalysts for the dry reforming of methane, J. Catal. 274 (2010) 11–20, https://doi.org/10.1016/J.JCAT.2010.05.020.
[161] A.S.A. Al-Fatish, A.A. Ibrahim, A.H. Fakeeha, M.A. Soliman, M.R.H. Siddiqui, A. E. Abasaeed, Coke formation during CO_2 reforming of CH4 over alumina-supported nickel catalysts, Appl. Catal. A: Gen. 364 (2009) 150–155, https://doi.org/10.1016/J.APCATA.2009.05.043.
[162] Y.H. Wang, H.M. Liu, B.Q. Xu, Durable Ni/MgO catalysts for CO_2 reforming of methane: Activity and metal–support interaction, J. Mol. Catal. A: Chem. 299 (2009) 44–52, https://doi.org/10.1016/J.MOLCATA.2008.09.025.
[163] Z. Alipour, M. Rezaei, F. Meshkani, Effects of support modifiers on the catalytic performance of Ni/Al2O3 catalyst in CO_2 reforming of methane, Fuel 129 (2014) 197–203, https://doi.org/10.1016/J.FUEL.2014.03.045.
[164] M. Khajenoori, M. Rezaei, F. Meshkani, Dry reforming over CeO2-promoted Ni/MgO nano-catalyst: Effect of Ni loading and $CH4/CO_2$ molar ratio, J. Ind. Eng. Chem. 21 (2015) 717–722, https://doi.org/10.1016/J.JIEC.2014.03.043.
[165] N. Hadian, M. Rezaei, Combination of dry reforming and partial oxidation of methane over Ni catalysts supported on nanocrystalline MgAl2O4, Fuel 113 (2013) 571–579, https://doi.org/10.1016/J.FUEL.2013.06.013.
[166] H.V. Fajardo, A.O. Martins, R.M. De Almeida, L.K. Noda, L.F.D. Probst, N.L. V. Carreño, A. Valentini, Synthesis of mesoporous Al2O3 macrospheres using the biopolymer chitosan as a template: A novel active catalyst system for CO_2 reforming of methane, Mater. Lett. 59 (2005) 3963–3967, https://doi.org/10.1016/J.MATLET.2005.07.071.
[167] M. Rezaei, S.M. Alavi, S. Sahebdelfar, Z.F. Yan, Effects of CO_2 content on the activity and stability of nickel catalyst supported on mesoporous nanocrystalline zirconia, J. Nat. Gas. Chem. 17 (2008) 278–282, https://doi.org/10.1016/S1003-9953(08)60064-X.
[168] C. Shi, P. Zhang, Effect of a second metal (Y, K, Ca, Mn or Cu) addition on the carbon dioxide reforming of methane over nanostructured palladium catalysts, Appl. Catal. B: Environ. 115–116 (2012) 190–200, https://doi.org/10.1016/J.APCATB.2011.12.002.
[169] J.D.A. Bellido, E.M. Assaf, Effect of the Y2O3–ZrO2 support composition on nickel catalyst evaluated in dry reforming of methane, Appl. Catal. A: Gen. 352 (2009) 179–187, https://doi.org/10.1016/J.APCATA.2008.10.002.
[170] F. Pompeo, N.N. Nichio, O.A. Ferretti, D. Resasco, Study of Ni catalysts on different supports to obtain synthesis gas, Int. J. Hydrog. Energy 30 (2005) 1399–1405, https://doi.org/10.1016/J.IJHYDENE.2004.10.004.
[171] J. Xu, W. Zhou, Z. Li, J. Wang, J. Ma, Biogas reforming for hydrogen production over nickel and cobalt bimetallic catalysts, Int. J. Hydrog. Energy 34 (2009) 6646–6654, https://doi.org/10.1016/J.IJHYDENE.2009.06.038.
[172] L. Qian, Z. Ma, Y. Ren, H. Shi, B. Yue, S. Feng, J. Shen, S. Xie, Investigation of La promotion mechanism on Ni/SBA-15 catalysts in CH4 reforming with CO_2, Fuel 122 (2014) 47–53, https://doi.org/10.1016/J.FUEL.2013.12.062.
[173] D. Liu, W.N.E. Cheo, Y.W.Y. Lim, A. Borgna, R. Lau, Y. Yang, A comparative study on catalyst deactivation of nickel and cobalt incorporated MCM-41 catalysts modified by platinum in methane reforming with carbon dioxide, Catal. Today 154 (2010) 229–236, https://doi.org/10.1016/J.CATTOD.2010.03.054.
[174] I. Cohen, Y. Huang, J. Chen, J. Benesty, J. Benesty, J. Chen, Y. Huang, I. Cohen, Pearson correlation coefficient, Noise Reduct. Speech Process. (2009) 1–4.
[175] J. Li, L. Pan, M. Suvarna, X. Wang, Machine learning aided supercritical water gasification for H2-rich syngas production with process optimization and catalyst screening, Chem. Eng. J. 426 (2021), 131285, https://doi.org/10.1016/j.cej.2021.131285.
[176] Y. Dong, Y. Zhang, M. Ran, X. Zhang, S. Liu, Y. Yang, W. Hu, C. Zheng, X. Gao, Accelerated identification of high-performance catalysts for low-temperature NH 3 -SCR by machine learning, J. Mater. Chem. A 9 (2021) 23850–23859, https://doi.org/10.1039/d1ta06772a.
[177] K. Vellayappan, Y. Yue, K.H. Lim, K. Cao, J.Y. Tan, S. Cheng, T. Wang, T.Z. H. Gani, I.A. Karimi, S. Kawi, Impacts of catalyst and process parameters on Ni-catalyzed methane dry reforming via interpretable machine learning, Appl. Catal. B: Environ. 330 (2023), 122593, https://doi.org/10.1016/j.apcatb.2023.122593.
[178] M. Suvarna, T.P. Araújo, J. Pérez-Ramírez, A generalized machine learning framework to predict the space-time yield of methanol from thermocatalytic CO_2 hydrogenation, Appl. Catal. B: Environ. (2022), 121530.
[179] J. Abdi, M. Hadipoor, F. Hadavimoghaddam, A. Hemmati-Sarapardeh, Estimation of tetracycline antibiotic photodegradation from wastewater by heterogeneous metal-organic frameworks photocatalysts, Chemosphere 287 (2022), 132135, https://doi.org/10.1016/J.CHEMOSPHERE.2021.132135.
[180] L. Prokhorenkova, G. Gusev, A. Vorobev, A.V. Dorogush, A. Gulin, CatBoost: unbiased boosting with categorical features, Adv. Neural Inf. Process. Syst. 31 (2018).
[181] CatBoost, CatBoost training parameter, (n.d.). https://catboost.ai/en/docs/references/training-parameters/.
[182] H. Jabbar, R.Z. Khan, Methods to avoid over-fitting and under-fitting in supervised machine learning (comparative study), Comput. Sci., Commun. Instrum. Devices 70 (2015).
[183] S.L. Brunton, B.R. Noack, P. Koumoutsakos, Machine learning for fluid mechanics, Annu. Rev. Fluid Mech. 52 (2020) 477–508.
[184] T.N. Nguyen, T.T.P. Nhat, K. Takimoto, A. Thakur, S. Nishimura, J. Ohyama, I. Miyazato, L. Takahashi, J. Fujima, K. Takahashi, High-throughput experimentation and catalyst informatics for oxidative coupling of methane, ACS Catal. 10 (2019) 921–932.
[185] H. Nguyen-Phu, T. Kim, Y. Kim, K.H. Kang, H. Cho, J. Kim, I. Ro, Role of phase in NiMgAl mixed oxide catalysts for CO_2 dry methane reforming (DRM), Catal. Today 411–412 (2023), 113894, https://doi.org/10.1016/j.cattod.2022.08.036.
[186] Y. Ogura, T. Asai, K. Sato, S. Miyahara, T. Toriyama, T. Yamamoto, S. Matsumura, K. Nagaoka, Effect of calcination and reduction temperatures on the catalytic activity of Ru/La0. 5Ce0. 5O1. 75 for ammonia synthesis under mild conditions, Energy Technol. 8 (2020) 2000264.